BIOCHEMISTRY
including biophysical chemistry & molecular biology

Article

pubs.acs.org/biochemistry

Remarkable Stabilization of Plasminogen Activator Inhibitor 1 in a "Molecular Sandwich" Complex

Galina Florova,[†] Sophia Karandashova,[†] Paul J. Declerck,[‡] Steven Idell,[†] and Andrey A. Komissarov*[,†]

[†]Texas Lung Injury Institute, University of Texas Health Science Center at Tyler, 11937 U.S. Highway 271, Tyler, Texas 75708-3154, United States

[‡]Laboratory for Pharmaceutical Biology, Faculty of Pharmaceutical Sciences, Katholieke Universiteit Leuven, Leuven, Belgium

ABSTRACT: Plasminogen activator inhibitor 1 (PAI-1) levels are elevated in a number of life-threatening conditions and often correlate with unfavorable outcomes. Spontaneous inactivation due to active to latent transition limits PAI-1 activity *in vivo*. While endogenous vitronectin (Vn) stabilizes PAI-1 by 1.5−2.0-fold, further stabilization occurs in a "molecular sandwich" complex (MSC) in which a ligand that restricts the exposed reactive center loop is bound to PAI-1/Vn. The effects of S195A two-chain urokinase (tcuPA) and Vn on inactivation of wild-type (wt) glycosylated (Gl-PAI-1), nonglycosylated (rPAI-1), and nonglycosylated Q123K PAI-1 (lacks Vn binding) forms were studied. S195A tcuPA decreased the rate constant (k_L) for spontaneous inactivation at 37 °C for rPAI-1, Q123K, and Gl-PAI-1 by 6.7-, 3.4-, and 7.8-fold, respectively, and both S195A tcuPA and Vn by 66.7-, 5.5-, and 103.3-fold, respectively. Analysis of the temperature dependences of k_L revealed a synergistic increase in the Gibbs free activation energy for spontaneous inactivation of wt Gl-PAI-1 and rPAI-1 in MSC from 99.8 and 96.1 to 111.3 and 107.0 kJ/mol, respectively, due to an increase in the activation enthalpy and a decrease in the activation entropy. Anti-PAI-1 monoclonal antibodies (mAbs) competing with proteinase also stabilize PAI-1/Vn. The rate of inhibition of target proteinases by MSCs, with a stoichiometry close to unity, was limited by the dissociation (k = 10^{-4} to 10^{-3} s^{-1}) of S195A tcuPA or mAb. The stabilization of PAI-1 in MSCs *in vivo* may potentiate uncontrolled thrombosis or extravascular fibrin deposition, suggesting a new paradigm for using PAI-1 inhibitors and novel potential targets for therapy.

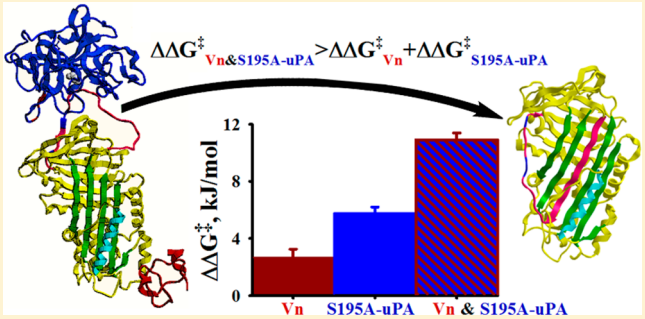

Plasminogen activator inhibitor 1 (PAI-1) is a major endogenous inhibitor of tissue-type (tPA) and urokinase-type (uPA) plasminogen activators, contributes to the regulation of normal and pathological thrombolysis and fibrinolysis and cell migration, and participates in multiple signaling pathways.[1−4] Because elevated plasma levels of PAI-1 antigen[5−8] and activity[8−10] correlate with severity and unfavorable outcomes in a number of diseases, PAI-1 is considered a biomarker and potential molecular target for therapeutics.

Mechanism-based inhibition of proteinases by PAI-1 (Scheme 1) starts by binding the enzyme at the docking site, resulting in the formation of a Michaelis complex (MC). Next, the cleavage of the scissile bond of the reactive center loop (RCL) of PAI-1 and the formation of an acyl-enzyme trigger massive conformational changes, resulting in the rapid insertion of the RCL (k_{lim1}) as strand 3 into central β-sheet A, and the translocation of the bound enzyme to the opposite pole of PAI-1 (Scheme 1). Mechanical distortion of the native structure of the enzyme results in its stabilization, forming an inhibitory complex [SIC (Scheme 1)]. Proteinases differ in the rate of RCL insertion [k_{lim1} (Scheme 1)], which limits the rate of inhibition of the enzyme by PAI-1. The stoichiometry of inhibition, the number of PAI-1 molecules required to inhibit one molecule of the enzyme,[11] is close to unity for the reactions with tPA and uPA. Active PAI-1 is a kinetically trapped, metastable conformation of the serpin, which spontaneously converts to a thermodynamically stable, inactive, latent PAI-1 (Scheme 1). The slow transition of PAI-1 to its latent conformation caused by the spontaneous insertion of uncleaved RCL to the β-sheet A [k_{L1} (Scheme 1)] prevents accumulation of active PAI-1 and limits its endogenous activity. Under physiological conditions, the active conformation of PAI-1 has a short half-life ($t_{1/2}$), ranging between 1.5 and 2.0 h.[12]

Vitronectin (Vn), a cell adhesive glycoprotein, approaches micromolar levels in the circulation and binds active PAI-1 with nanomolar affinity [k_{-2}/k_{+2} < 10^{-8} M (Scheme 1)].[13−15] Vn stabilizes the active conformation of PAI-1, decreasing its rate of spontaneous inactivation [k_{L1}/k_{L2} = 1.5−2.0 (Scheme 1)].[16,17] Vn dissociates from PAI-1 after the insertion of its RCL (Scheme 1).[18] Binding Vn induces conformational changes in the proteinase docking site, which further facilitate interactions between the RCL and the active site of the target enzyme[19] because of an increase in the rigidity of the PAI-1 molecule.[20] The mechanism of inhibition of the enzyme by

Received: January 22, 2013
Revised: June 4, 2013
Published: June 4, 2013

Scheme 1. A Transient Ternary "Molecular Sandwich" Complex (MSC) Is a Part of the PAI-1 Inhibitory Mechanism *in vivo*[a]

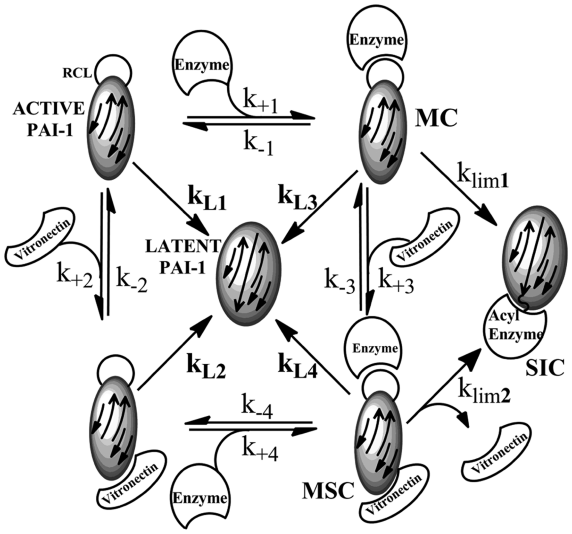

[a]Mechanism-based inactivation of the enzyme by PAI-1 and PAI-1/Vn results in a stable inhibitory complex (SIC). Formation of the acyl-enzyme from a Michaelis complex (MC) or MSC triggers fast insertion (k_{lim1} or k_{lim2}, respectively) of the reactive center loop (RCL) into central β-sheet A (arrows) as strand 3A (central arrow), translocation of the enzyme to the opposite pole of the PAI-1 molecule, and stabilization of the acyl-enzyme as the SIC. A decrease in k_{lim2} ($k_{lim2} = 0$ for S195A tcuPA) results in a stable ternary MSC (k_{+n} and k_{-n} are association and dissociation rate constants, respectively). Inactive, latent PAI-1 forms because of the slow spontaneous insertion of RCL into central β-sheet A (k_{L1}, k_{L2}, k_{L3}, and k_{L4} for free PAI-1, PAI-1 in the presence of Vn, S195A tcuPA, and both ligands, respectively).

PAI-1/Vn includes the formation of a transient ternary "molecular sandwich" complex (MSC) (Scheme 1). Vn often affects both the kinetics and stoichiometry of inhibition[21−29] for the reactions of PAI-1 with different enzymes. Binding Vn decreases the rate of RCL insertion [$k_{lim1} > k_{lim2}$ (Scheme 1)] for tcuPA, trypsin, and tctPA at pH <7.0[26,27] but does not affect the stoichiometry of inhibition.[24,26] Such a decrease in the limiting rate of RCL insertion (Scheme 1) reflects the stabilization of the ternary MSC, which, due to the abundance of endogenous Vn, is a part of the PAI-1 mechanism *in vivo*. A further decrease in k_{lim2} [stabilization of MSC (Scheme 1)] was observed for the reactions of PAI-1/Vn with activated protein C[25,28] and factor VIIa/tissue factor[29] [for both $k_{lim2} \ll k_{lim2}$ for target proteinases (Scheme 1)]. Thus, transient MSCs with different stabilities occur *in vivo* and could contribute to normal and pathological fibrinolysis and cell signaling.

Finally, inactive proteinases such as anhydrotrypsin (trypsin with dehydroalanine at position 195, chymotrypsin numbering) and S195A mutant variants of tPA and uPA,[30−32] when bound to PAI-1/Vn, form a stable MSC [$k_{lim2} = 0$ (Scheme 1)]. While binding Vn [k_{+2} (Scheme 1)] and inactive proteinases [k_{+1} (Scheme 1)] are among the mechanisms that stabilize active PAI-1 [$k_{L1} > k_{L2}$, and $k_{L1} > k_{L3}$ (Scheme 1)],[2,4] to the best of our knowledge, there is a lack of data about the stability of the active conformation of PAI-1 in stable [$k_{lim2} = 0$ (Scheme 1)] MSCs [k_{L4} (Scheme 1)]. A model of the MSC (Figure 1) based on known X-ray structures of active PAI-1 bound to S195A tcuPA[32] and the somatomedin B (SMB) domain of Vn[33] shows ligands bound to opposite poles of the PAI-1 molecule. Here

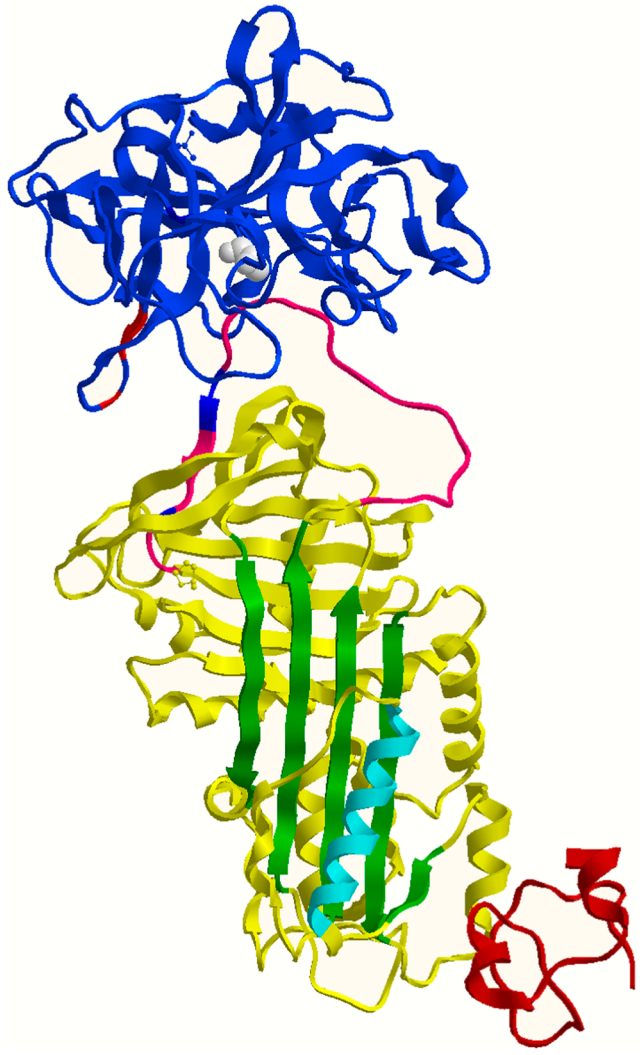

Figure 1. Proposed ribbon model of the S195A tcuPA/PAI-1/Vn molecular sandwich complex. Crystal structures of PAI-1 (yellow) complexes with S195A tcuPA (blue)[32] and the SMB domain of Vn (brown)[33] were used. The exposed RCL of active PAI-1 is colored red with positions of E350 and E351 (P4′P5′ nomenclature of Schechter and Berger[49]) colored blue, β-sheet A colored green, and α-helix F colored cyan. Active site A195 of S195A tcuPA is shown as a white space-filled residue, and positions of positively charged residues of the 37-loop of uPA are colored red.

we demonstrate that S195A, tcuPA, and Vn synergistically stabilize the active conformation of PAI-1, increasing the $t_{1/2}$ for its spontaneous inactivation up to almost 2 orders of magnitude. Moreover, we demonstrate that anti-PAI-1 monoclonal antibodies (mAbs), which compete for PAI-1 with proteinase,[34] also stabilize active PAI-1.

EXPERIMENTAL PROCEDURES

Proteins and Reagents. Monomeric Vn, wt nonglycosylated PAI-1 (rPAI-1), glycosylated PAI-1 (Gl-PAI-1), nonglycosylated Q123K PAI-1 (lacks vitronectin binding), and three mutant variants of PAI-1 with introduced cysteines labeled with *N*-{[2-(iodoacetoxy)ethyl]-*N*-methyl}amino-7-nitrobenz-2-oxa-3-diazole (NBD) [S338C (NBD P9) PAI-1, M447C (NBD P1′) PAI-1, and S119C (NBD S119C) PAI-1] were purchased from Molecular Innovations (Novi, MI). E350A/E351A NBD P9 PAI-1 was obtained and characterized

dx.doi.org/10.1021/bi400470s | *Biochemistry* 2013, 52, 4697−4709

as previously described.[35] S356A (S195A in chymotrypsin numbering) recombinant catalytically inactive scuPA was generated and purified, as previously described.[36,37] The proenzyme was converted to the two-chain form by incubation with the resin with immobilized plasmin (Molecular Innovations) as previously described.[38] Complete activation was confirmed via sodium dodecyl sulfate−polyacrylamide gel electrophoresis (SDS−PAGE) under reducing conditions, as described in ref 37. The urokinase activity standard (100000 IU/mg) was from American Diagnostica (Stanford, CT). Recombinant tcuPA was a gift from Abbott Laboratories (Chicago, IL). Recombinant single-chain tPA (sctPA) (Activase) was from Genentech (San Francisco, CA). Glu-plasminogen (Plg), plasmin (PL), and fluorogenic PL substrate were from Haematologic Technologies Inc. (HTI, Essex Junction, VT). Fluorogenic tPA and uPA substrates were from Centerchem Inc. (Norwalk, CT). All experiments were conducted in 20 mM Hepes/NaOH buffer (pH 7.4) containing 0.13 M NaCl.

Effects of S195A tcuPA and Anti-PAI-1 mAbs on the Spontaneous Inactivation of PAI-1 and PAI-1/Vn. Time-dependent spontaneous inactivation of rPAI-1, Q123K PAI-1, Gl-PAI-1, and their complexes with Vn, S195A tcuPA, anti-PAI-1 mAbs MA-56A7C10, MA-42A2F6, and MA-44E4, and two ligands (MSC formed in the presence of Vn and either S195A tcuPA or mAb) was studied by incubating the serpins (0.25−2.5 μM) with one or two ligands taken at a 1.0−2.0-fold molar excess in 20 mM Hepes/NaOH buffer (pH 7.4) containing 0.13 M NaCl at 37 °C for 0−720 h. The concentration of active PAI-1 was determined by two independent methods as previously described.[9,39] First, active PAI-1 in aliquots withdrawn at 0−168 h was titrated with increasing amounts of sctPA or tcuPA with a known specific activity, followed by measuring the residual tPA or uPA amidolytic activity. The concentration of active PAI-1 in aliquots was determined from the linear calibration plots obtained from the titration of known amounts of active PAI-1 with the same standard solutions of sctPA or tcuPA.[9,39] The same aliquots were incubated with a 1.2−2.5-fold molar excess (over PAI-1) of sctPA for 30−60 min at 37 °C followed with analysis of the reaction products by SDS−PAGE [NuPAGE Novex 4−12% Bis-Tris Midi gels (Invitrogen, Grand Island, NY)]. Proteins were visualized by being stained with SYPRO Ruby protein gel stain (Invitrogen). To estimate the level of active PAI-1, gels were scanned and analyzed using a Molecular Imager equipped with Quantity One (version 4.2.3) (Bio-Rad Laboratories, Hercules, CA). The amounts of PAI-1 {latent, cleaved, and in a complex with proteinase [SIC (Scheme 1)]} were estimated from the intensity of the corresponding bands, and active PAI-1 (50% of the density in SIC) was expressed as percent of the total PAI-1 density. After incubation for 1 month (720 h) at 37 °C, the PAI-1 activity was determined by two independent methods with higher levels of sensitivity: (i) PAI-1 inhibition of tcuPA-mediated Plg activation and (ii) visualization of PAI-1 at the gel [PAI-1/tPA complex (SIC), latent PAI-1, and cleaved PAI-1] by Western blotting using IBlot (Invitrogen) as described previously.[9,39]

Measurement of tPA, uPA, and PL Amidolytic Activity. Amidolytic activities of tPA and uPA were estimated from the time increase in fluorescence emission at 440 nm (excitation at 344 nm) of 0.2 mM fluorogenic substrates [Pefafluor tPA CH_3-SO_2-D-Phe-Gly-Arg-AMC AcOH and Pefafluor uPA Bz-β-Ala-Gly-Arg-AMC AcOH, respectively, where AMC is 7-amino-4-methylcoumarin (Centerchem Inc.)]. The PL activity was measured using fluorogenic substrate [D-Ala-Phe-Lys-ANS-NH-iC_4H_9·2HBr, where ANS is 6-amino-1-naphthalenesulfonamide (HTI)] and calculated from an increase in fluorescence emission at 470 nm (excitation at 352 nm) as previously described.[9,37,39] Amidolytic activity was measured in either white or black 96-well flat bottom plates from Costar (Corning Inc., Corning, NY) using a Varian Cary Eclipse fluorescence spectrophotometer (Varian Inc.) or Synergy HT Hybrid Reader (BioTek, Winooski, VT), respectively.

Stoichiometry of Inhibition for Inhibition of uPA and tPA by MSC. The stoichiometry of inhibition is the number of moles of PAI-1 required for the inactivation of 1 mol of proteinase.[11] The effects of binding of S195A tcuPA alone and with Vn on the stoichiometry of inhibition for tPA and uPA were determined directly by titration of binary complexes (S195A tcuPA/PAI-1 variant) and MSCs (Scheme 3) with proteinase using a Varian Cary Eclipse fluorescence spectrophotometer. Briefly, the known amount (20−100 nM) of binary or ternary complex was incubated with increasing amounts of the proteinase for 30 min at 37 °C. A residual enzyme activity was determined using the fluorogenic substrate as previously described.[37,40] If we start from the equivalence point (complete neutralization of the PAI-1 variant), the addition of proteinase resulted in measurable (limit of detection of 0.1 nM) enzymatic activity. The stoichiometry of inhibition for complexes with NBD P9 PAI-1 was determined as described previously.[41] The values of the stoichiometry of inhibition (average of two or three experiments) were calculated as a ratio of moles of active PAI-1 in the complex to moles of the proteinase used to reach the equivalence point. The stoichiometries of inhibition for the reaction of a 1.2−2.5-fold molar excess of tPA or uPA and rPAI-1, Gl-PAI-1, Q123K PAI-1, and their complexes with S195A tcuPA, Vn, or both ligands were also estimated from SDS−PAGE analysis as described previously.[9,39,41]

Kinetics of Formation and Dissociation of MSC. NBD P1′, NBD S119C, and NBD P9 mutant variants of PAI-1 were used to measure the second-order association rate constants [k_{+1}, k_{+2}, k_{+3}, and k_{+4} (Scheme 1)] for the formation of MSC and binary complexes using stopped-flow fluorimetry as previously described.[26,41,31] An NBD PAI-1 variant (or its complex with one ligand, at 10−50 nM) was mixed with increasing concentrations of the ligand (second ligand) in a microvolume stopped-flow reaction analyzer [model SX-20 (Applied Photophysics Ltd., Leatherhead, U.K.)], equipped with a fluorescence detector and a thermostated (25 °C) cell. The progress of the reaction was monitored as an increase in the NBD fluorescence emission via a 515 nm cutoff filter (excitation at 490 nm). Pro-Data Viewer (Applied Photophysics Ltd.) was used to fit a single-exponential equation ($F_t = F_\infty + A_1 \times e^{-k_{obs}t}$) to the data (where k_{obs} is the first-order rate constant of complex formation and F_t, F_∞, and A are fluorescence emission at time t, at infinite time, and the amplitude, respectively). Diffusion-limited association rate constants [k_{+1}, k_{+2}, k_{+3}, and k_{+4} (Scheme 1)] were determined from the slopes of linear k_{obs} with ligand concentration using SigmaPlot version 11.0 (SPSS Inc., San Jose, CA). Dissociation rate constants [k_{-1} and k_{-4} (Scheme 1)] for complexes of NBD P1′, NBD P9, and P4′P5′/AA NBD P9 PAI-1 variants with S195A tcuPA were determined in a manner similar to that described previously for the reaction between PAI-1 and

dx.doi.org/10.1021/bi400470s | Biochemistry 2013, 52, 4697−4709

prourokinase.[37] Briefly, preformed complexes were rapidly mixed with an excess of tcuPA or sctPA in the SX-20 instrument, and the progress of the reaction was monitored via changes in the NBD fluorescence emission with time. The values of k_{obs} were calculated by fitting a single-exponential equation to the data and plotted versus proteinase concentration. The linear equation $k_- = k_{obs}$ (where k_- values are k_{-1} and k_{-4}) was fit to the data using SigmaPlot version 11.0 (SPSS Inc.). The values of k_{-1} and k_{-4} for unlabeled variants of PAI-1 (wt rPAI-1, Gl-PAI-1, and Q123K PAI-1) were determined using the competition of NBD P1′ PAI-1 with unlabeled variants for S195A tcuPA. Briefly, preformed complexes of unlabeled PAI-1 variants (5−20 nM) with a 1.0−1.2-fold molar excess of S195A tcuPA were mixed with NBD P1′ PAI-1 (40−250 nM) using the SX-20 instrument; values of k_{obs} were calculated from changes in the NBD fluorescence emission with time, plotted versus NBD P1′ PAI-1 concentration, and the linear equation $k_- = k_{obs}$ (where k_- values are k_{-1} and k_{-4}) was fit to the data using SigmaPlot version 11.0 (SPSS Inc.).

The affinities of PAI-1 and its variants (with or without Vn present) to S195A tcuPA were determined in a manner similar to that described for anti-PAI-1 mAbs.[41] The affinity of S195A tcuPA for NBD P9 PAI-1 was estimated from the dependence of k_{obs} for the reaction of tctPbA with 0.5−5.0 nM NBD P9 PAI-1 (NBD P9 PAI-1/Vn) preincubated for 15 min with increasing amounts of S195A tcuPA. The affinity of wt r-PAI-1, Gl-PAI-1, and Q123K PAI-1 was estimated from the dependences of the initial rates of amidolytic activity of tPA on the concentration of S195A tcuPA after mixing of 0.5−5 nM PAI-1 or its variants preincubated for 15 min with increasing amounts of S195A tcuPA (with or without Vn) with an equimolar amount of tctPA and Pefafluor tPA (0.2 mM).

Interaction of NBD P1′ PAI-1 with tcuPA. The simplest mechanism of the reaction between serpin (I) and proteinase (E) (Scheme 2) includes the Michaelis complex (E·I), followed

Scheme 2. Two-Step Inactivation of Proteinase (E) by PAI-1 (I)

$$E + I \underset{k_{-1}}{\overset{k_1}{\rightleftharpoons}} E{\cdot}I \xrightarrow{k_{lim}} E\text{-}I^*$$

by the formation of a stable inhibitory complex (E-I*). A change in the fluorescence emission of the P1′ NBD group reports both the formation of the Michaelis complex [an increase in the NBD fluorescence emission (Figure 3, inset)] and the dissociation of the enzyme from the initial docking site due to RCL insertion (a decrease in the NBD fluorescence emission).[31] The two corresponding values of k_{obs} were calculated by fitting a double-exponential equation ($F_t = F_\infty + A_1e^{-(kobs1)t} + A_2e^{-(kobs2)t}$) using Pro-Data Viewer (Applied Photophysics Ltd.) to the recorded changes in the P1′ NBD fluorescence.

k_{lim} and K_M were calculated by fitting the dependence of k_{obs1} on enzyme concentration with the hyperbolic equation $k_{obs1} = k_{lim}[E]/(K_M + [E])$ [where k_{lim} is the first-order rate constant at an infinite concentration of the enzyme and $K_M = (k_{lim} + k_{-1})/k_1$ is the concentration of the enzyme at $k_{obs1} = k_{lim}/2$] as described previously.[26,41] k_{+1} and k_{-1} (Scheme 2) were calculated by fitting the linear equation $k_{obs2} = k_{lim} + k_{-1} + k_1[E]$ to the linear dependence of the fast k_{obs2} on the enzyme concentration as described previously.[31]

Effects of Temperature on the Rate of Spontaneous RCL Insertion Due to the Active to Latent Transition of PAI-1 Variants and Their Complexes with Vn and S195A tcuPA. The temperature dependences (37−60 °C) of k_{L1}, k_{L2}, k_{L3}, and k_{L4} (Scheme 1) for rPAI-1, Gl-PAI-1, and Q123K PAI-1 and their complexes with Vn, S195A tcuPA, and both ligands were analyzed as Eyring plots of $\ln(k_L/T)$ or versus $1/T$. The values of k_{L1}, k_{L2}, k_{L3}, and k_{L4} (Scheme 1) for rPAI-1, Gl-PAI-1, and Q123K PAI-1 and their complexes with Vn, S195A tcuPA, and both ligands were measured at 37, 50, 55, and 60 °C. The activation enthalpy ($\Delta H^‡$) and entropy ($\Delta S^‡$) were determined from the Eyring plots of $\ln(k_L/T)$ or versus $1/T$, which linearly relates both parameters: $\ln(k_L/T) = \ln(k_B/h) + \Delta S^‡/R - \Delta H^‡/RT$, where T is the absolute temperature and R, k_B, and h are 8.3145 J/mol, 1.3806×10^{-23} J/K, and 6.626×10^{-34} J/s, respectively. The parameters of the best fit of the linear equation to the data [SigmaPlot version 11.0 (SPSS Inc.)] were used to calculate $\Delta H^‡$ and $\Delta S^‡$ as −(slope) × 8.3145 J/mol and (intercept − 23.76) × 8.3145 J mol^{-1} K^{-1}, respectively. The values of the Gibbs free activation energy ($\Delta G^‡$) for the spontaneous active to latent transition of PAI-1 variants and their complexes were calculated with the equation $\Delta G^‡ = \Delta H^‡ - T\Delta S^‡$. To evaluate the dependence between contributions of $\Delta H^‡$ and $\Delta S^‡$ to $\Delta G^‡$ for spontaneous inactivation of wt Gl-PAI-1, rPAI-1, and Q123K PAI-1 alone or in the presence of Vn, S195A tcuPA, or both ligands, the values of $\Delta H^‡$ were plotted as a function of $-T\Delta S^‡$. A linear equation was fit to the data using SigmaPlot version 11.0 (SPSS Inc.).

Additivity in the Effects of S195A tcuPA and Vn on the Active to Latent Transition of PAI-1. The additivity in the effects of Vn and S195A tcuPA on the spontaneous inactivation of PAI-1 variants was tested by comparing changes in the $\Delta G^‡$ ($\Delta\Delta G^‡$) caused by Vn ($\Delta\Delta G^‡_{Vn}$), S195A tcuPA ($\Delta\Delta G^‡_{S195A\ tcuPA}$), and both ligands together ($\Delta\Delta G^‡_{Vn/S195A\ tcuPAl}$); assuming additivity if $\Delta\Delta G^‡_{Vn/S195A\ tcuPAl} = \Delta\Delta G^‡_{Vn} + \Delta\Delta G^‡_{S195A\ tcuPA}$ and if $\Delta\Delta G^‡_{Vn/S195A\ tcuPAl} > \Delta\Delta G^‡_{Vn} + \Delta\Delta G^‡_{S195A\ tcuPA}$, the effect is synergistic. The values of $\Delta\Delta G^‡$ are presented as a bar graph.

Effects of MSC on the Acceleration of the Active to Latent Transformation by mAb MA-33B8. NBD P9 PAI-1 (10−20 nM) and its complexes with Vn (20−50 nM), MSC with S195A tcuPA (20−50 nM), or 20−50 nM mAb MA-56A7C10, MA-42A2F6, or MA-44E4 were incubated with MA-33B8 (50−400 nN) in 96-well flat bottom plates from Costar (Corning Inc.), and increases in NBD fluorescence with time were measured using a fluorescence spectrophotometer Synergy HT Hybrid Reader (BioTek). The k_{obs} values were calculated by fitting a single-exponential equation to the data using Gen5 version 2.0 (BioTek) and SigmaPlot version 11.0 (SPSS Inc.), as described elsewhere,[26,41,42] and plotted against the concentration of MA-33B8.[43]

Data Analysis. Pro-Data Viewer (Applied Photophysics Ltd.) was used to analyze stopped-flow fluorescence traces. All of the measurements were taken under pseudo-first-order kinetic conditions (the concentration of the ligand or proteinase was at least 5-fold higher than that of a PAI-1 variant or its complexes). The values of the correlation coefficient ($r^2 > 0.90$ for all of the kinetic data) and visual analysis of the plots of the residuals (deviation of the fitted function from the actual data) were used to estimate the quality of the fit. The values of k_{obs} (average of four to six measurements, standard error of <10%) were plotted against the molar concentration of proteinase or ligand.

dx.doi.org/10.1021/bi400470s | Biochemistry 2013, 52, 4697−4709

Table 1. Values of the Association (k_{+1}, k_{+2}, k_{+3}, and k_{+4}) and Dissociation (k_{-1}, k_{-2}, k_{-3}, and k_{-4}) Rate Constants and Dissociation Equilibrium Constants ($K_D = k_-/k_+$) for the Interactions among wt PAI-1, Its Mutant Variants, and Their Complexes with S195A tcuPA and Vn at 25 °C

	ligand	PAI-1 variant	k_+ (μM^{-1} s^{-1})	k_- ($\times 10^{-3}$ s^{-1})	$K_D = k_-/k_+$ (nM)
k_{+1}	S195A	wt rPAI-1	5.4[a]	7.0 ± 0.4[b]	1.3 ± 0.4[c]
	tcuPA	Gl-PAI-1	4.2[a]	5.0 ± 0.3[b]	1.2 ± 0.5[c]
		Q123K PAI-1	4.6[a]	6.0 ± 0.4[b]	1.3 ± 0.5[c]
		NBD P9 PAI-1	7.3 ± 0.2[d]	6.0 ± 0.3[e]	1.2 ± 0.6[f]
		NBD P1′ PAI-1	6.1 ± 0.2[d]	150 ± 20[e]	24.6[g]
		NBD S119C PAI-1	5.0 ± 0.2[d]	ND[h]	ND[h]
		P4′P5′/AA NBD P9 PAI-1	2.8 ± 0.2[i]	7.0 ± 0.2[e]	2.5[g]
k_{+2}	Vn	NBD S119C PAI-1	7.2 ± 0.3[d]	2.2–7.2[a]	0.3–1.0[j]
k_{+3}	Vn	NBD S119C PAI-1	13.3 ± 0.3[d]	ND[h]	ND[h]
k_{+4}	S195A	wt rPAI-1	4.3[a]	3.0 ± 0.2[b]	0.7 ± 0.3[c]
	tcuPA	Gl-PAI-1	5.0[a]	4.0 ± 0.3[b]	0.8 ± 0.4[c]
		Q123K PAI-1[k]	4.6[a]	6.0 ± 0.3[b]	1.3 ± 0.3[c]
		NBD P9 PAI-1	8.0 ± 0.3[d]	4.0 ± 0.2[e]	0.9 ± 0.4[f]
		NBD P1′ PAI-1	4.0 ± 0.2[d]	90 ± 10[e]	22.5[g]
		NBD S119C PAI-1	5.0 ± 0.2[d]	ND[h]	ND[h]
		P4′P5′/AA NBD P9 PAI-1	ND[h]	4.0 ± 0.2[e]	ND[h]

[a]Estimated from K_D and k_{+1} and k_{+4} or k_{-1} and k_{-4} values. [b]Measured by the reaction of preformed unlabeled PAI-1 variant/ligand(s) complexes with an excess of NBD P1′ PAI-1. [c]Estimated from the dependence of the initial amidolytic activity of tPA after its reaction with an equimolar PAI-1 variant (its complex with Vn) incubated with increasing amounts of S195A tcuPA. [d]Determined from the slopes of linear dependences of k_{obs} vs ligand concentration for the interaction of NBD-labeled variants of PAI-1 (their complexes) with a corresponding ligand (Figure 2). [e]Determined from k_{obs} (independent of proteinase concentration) for the reaction of the preformed NBD PAI-1/ligand(s) complex with an excess of sctPA or tcuPA (Figure 2). [f]Determined from the dependence of k_{obs} on S195A tcuPA concentration for the reaction of an excess of tctPA with NDB P9 PAI-1 preincubated with different amounts of S195A tcPAI-1 as described previously.[41] [g]Calculated as k_-/k_+. [h]Not determined. [i]k_{+1} for association of P4′P5′/AA PAI-1 with tcuPA.[35] [j]K_D for binding of Vn to wt PAI-1.[33,67] [k]Q123K PAI-1 possesses a low affinity for Vn.[45]

RESULTS AND DISCUSSION

Formation and Dissociation of the MSC and Its Interaction with Target Proteinases (Scheme 1). Three mutant variants of PAI-1 [wild-type recombinant nonglycosylated (rPAI-1), glycosylated (Gl-PAI-1), which was recently shown to be more stable than rPAI-1,[44] and a nonglycosylated mutant variant that lacks Vn binding ability (Q123K PAI-1)[45]] were selected to compare the contribution of glycosylation and Vn binding to the stabilization of the active conformation of

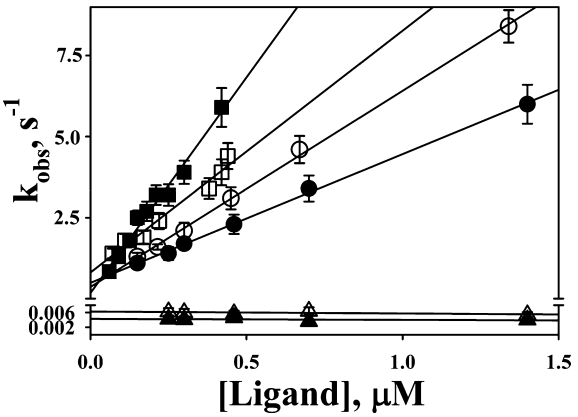

Figure 2. Rapid association of PAI-1 and ligands and slow dissociation of S195A tcuPA. Linear dependences of k_{obs} on ligand concentration for the association of PAI-1 and its complexes with ligands [k_{+n}; n = 1–4 (Scheme 1)]. Values of k_{+n} for the interaction of S195A tcuPA with NBD P1′ PAI-1 (○), Vn and NBD S119C PAI-1 (□), S195A tcuPA with NBD P1′ PAI-1/Vn (●), and Vn with NBD S119C PAI-1/S195A tcuPA (■) were calculated from the slopes of the best linear fit to the data (Table 1). Slow dissociation of S195A tcuPA limits the reaction between tPA and the complex of NBD P9 PAI-1 with S195A tcuPA (△) and MSC [complex of NBD P9 PAI-1 with S195A tcuPA and Vn (Scheme 1)] (▲).

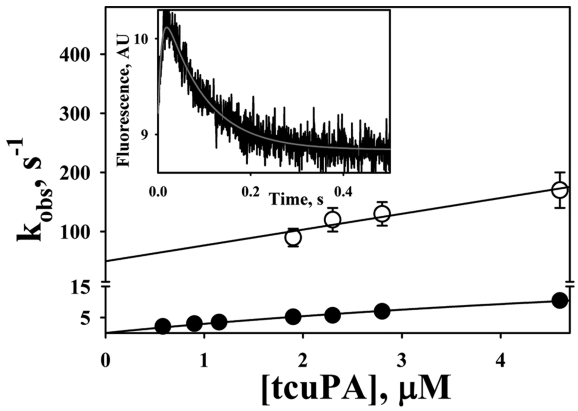

Figure 3. NBD-labeled cysteine at position P1′ of the RCL of PAI-1 affects the kinetics of inhibition of tcuPA. Dependences of the k_{obs} for the fast step (an increase in NBD fluorescence emission) (○) and slow step (a decrease in NBD fluorescence emission) (●) on enzyme concentration. The solid lines represent the best fits of the linear equation $k_{obs2} = k_{lim} + k_{-1} + k_1$[tcuPA] ($r^2 = 0.93$) (fast step) and the hyperbolic equation $k_{obs1} = (k_{lim}[\text{tcuPA}])/(K_m + [\text{tcuPA}])$ ($r^2 = 0.99$) (slow step) to the data by SigmaPlot version 11.0. The values of k_{lim} and K_m (Scheme 2) were 33.3 ± 5.2 s^{-1} and 10.2 ± 2.2 μM, respectively. The slope and intercept of the linear dependence of k_{obs} on enzyme concentration represent a second-order rate constant for the interaction of tcuPA with NBD P1′ PAI-1: k_{+1} = 26.8 ± 2.8 μM^{-1} s^{-1}, and $k_{lim} + k_{-1}$ = 50 ± 8 s^{-1}, respectively. The inset shows a trace of the changes in NBD fluorescence for the reaction of NBD P1′ PAI-1 (0.12 μM) with 2.0 μM tcuPA. Values of k_{obs1} and k_{obs2} were calculated by fitting (gray line) a double-exponential equation to the time traces of changes in NBD fluorescence emission using SigmaPlot version 11.0.

dx.doi.org/10.1021/bi400470s | Biochemistry 2013, 52, 4697–4709

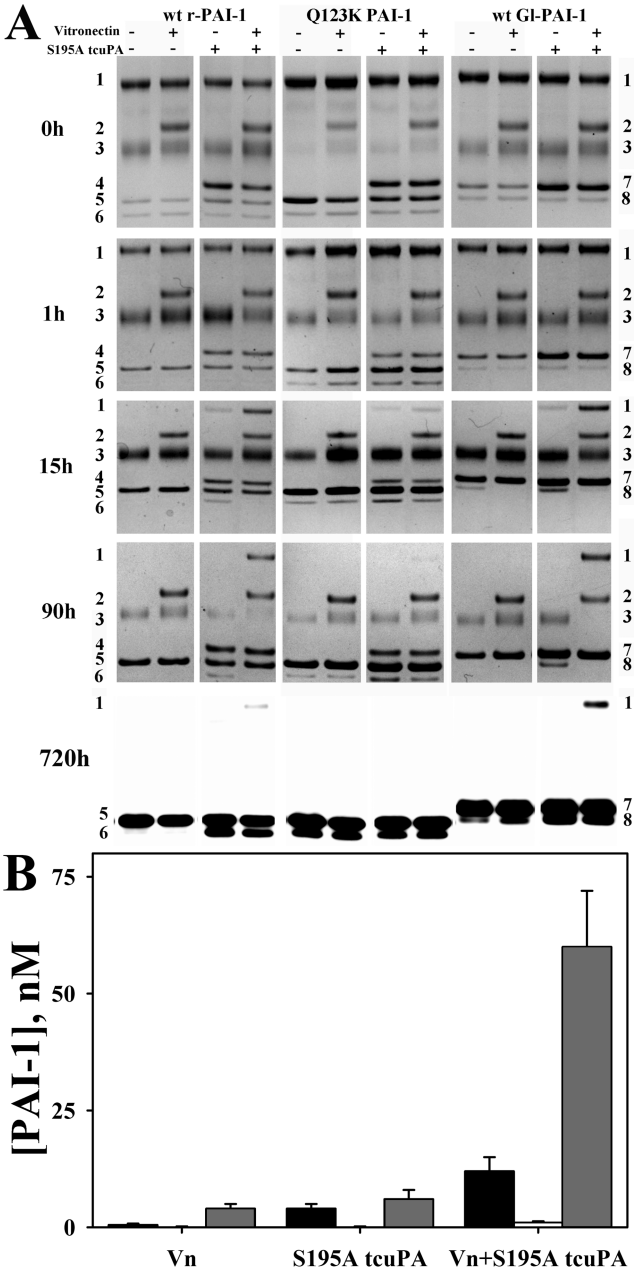

Figure 4. Tremendous stabilization of active PAI-1 in MSC under physiological conditions. (A) SDS−PAGE analysis of products of the reaction between sctPA and rPAI-1, Q123K PAI-1, and Gl-PAI-1 and their complexes with Vn, S195A tcuPA, and both ligands (the table at the top of the gels) incubated for 0, 1, 15, 90 (stained with SYRRO Ruby), and 720 h (PAI-1 antigen visualized via Western blot analysis) at 37 °C. Positions of PAI-1/tPA SIC (1), Vn (2), tPA (3), S195A tcuPA (4), latent and cleaved rPAI-1 (5 and 6, respectively), comigrating S195A tcuPA and latent Gl-PAI-1 (7), and cleaved Gl-PAI-1 (8) are indicated to the left (rPAI-1 and Q123K PAI-1) and right (Gl-PAI-1) of the gels. (B) Active PAI-1 concentration in the reaction mixtures, shown in the Western blot (A, bottom panel), estimated by inhibiting the activation of Plg by uPA, as described previously.[9,39] After incubation with both Vn and S195A tcuPA for 1 month (720 h) at 37 °C, rPAI-1 (black bars) and Gl-PAI-1 (gray bars), but not Q123K PAI-1 (white bars), inhibit the activation of Plg by uPA.

PAI-1 in MSCs. The kinetics of MSC formation among PAI-1, Vn, and S195A tcuPA (Figure 1 and Scheme 1) and its

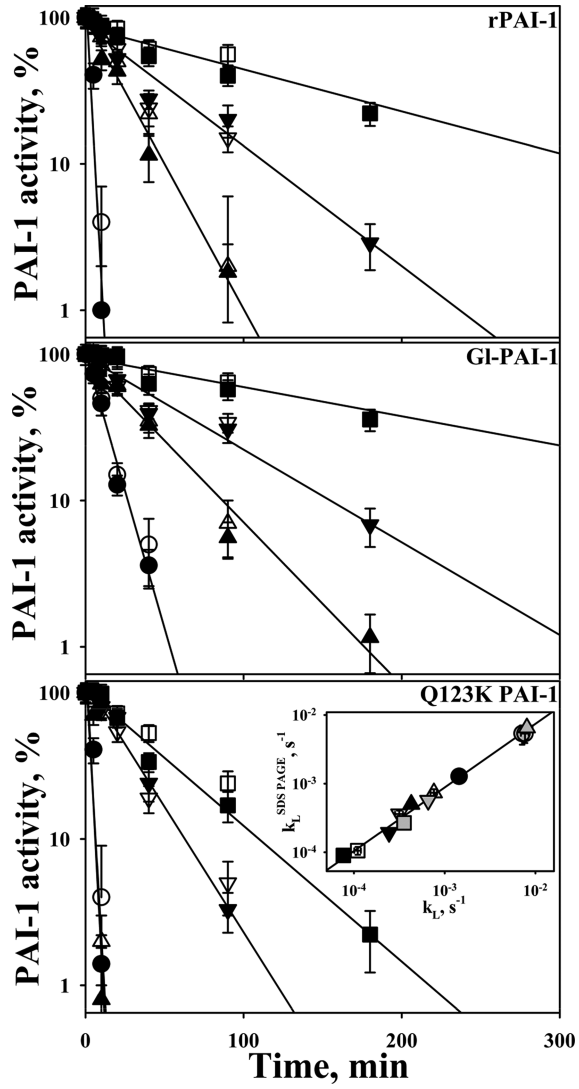

Figure 5. Spontaneous inactivation of rPAI-1, Q123K PAI-1, and Gl-PAI-1 (circles) and their complexes with Vn (triangles), S195A tcuPA (inverted triangles), and both ligands (squares) at 50 °C. The concentration of active PAI-1 was determined from the residual tPA amidolytic activity after titration of the sample with increasing amounts of sctPA as described in Experimental Procedures and plotted on a semilogarithmic scale (filled symbols). Separate aliquots were incubated with an excess of sctPA, and the products of the reaction were separated by SDS−PAGE, as shown in Figure 4 and described in Experimental Procedures. The amounts of active PAI-1 were estimated from the relative density of SIC and latent and cleaved PAI-1 on gels and plotted as empty symbols. Linear equations were fit to both sets of data (solid lines represent the best fits to filled symbols) using SigmaPlot version 11.0, and the first-order rate constants [k_{L1}, k_{L2}, k_{L3}, and k_{L4} (Table 2) and $k_{L1}^{SDS-PAGE}$, $k_{L2}^{SDS-PAGE}$, $k_{L3}^{SDS-PAGE}$, and $k_{L4}^{SDS-PAGE}$, respectively (Scheme 1)] were calculated from the slopes. The inset shows the correlation between values of k_L measured by two different methods. The values of k_L estimated from the results of SDS−PAGE analysis were plotted vs the corresponding values obtained from titration of the reaction mixtures with sctPA: rPAI-1 (empty symbols), Gl-PAI-1 (black symbols), and Q123K PAI-1 (gray symbols). Data for free rPAI-1, Gl-PAI-1, and Q123K PAI-1 are shown as circles, data for their complexes with Vn as triangles, data for their complexes with S195A tcuPA as inverted triangles, and data for both ligands as squares. The solid line represents the best linear fit to the data of the linear equation $k_L^{SDS-PAGE} = -0.27 + 0.93k_L$ ($r^2 = 0.99$).

dx.doi.org/10.1021/bi400470s | Biochemistry 2013, 52, 4697−4709

Table 2. Values of k_{L1}, k_{L2}, k_{L3}, and k_{L4} (Scheme 1) for rPAI-1, Q123K PAI-1, Gl-PAI-1, and Their Complexes with Vn, S195A tcuPA, and Both Ligands, Determined at Different Temperatures[a]

		k_L ($\times 10^{-3}$ s^{-1})			
PAI-1	T (°C)	none (k_{L1})	Vn (k_{L2})	S195A tcuPA (k_{L3})	Vn/S195A tcuPA (k_{L4})
rPAI-1	37	0.22 ± 0.03	0.13 ± 0.02	0.033 ± 0.004	0.0034 ± 0.0005
	50	7.7 ± 0.6	0.76 ± 0.06	0.32 ± 0.04	0.11 ± 0.02
	55	11.2 ± 1.5	1.9 ± 0.2	0.68 ± 0.08	0.12 ± 0.01
	60	24.6 ± 1.8	11.0 ± 1.5	3.2 ± 0.3	0.42 ± 0.03
Q123K PAI-1	37	0.17 ± 0.02	0.18 ± 0.02	0.050 ± 0.006	0.033 ± 0.005
	50	7.1 ± 1.4	8.1 ± 1.4	0.66 ± 0.07	0.36 ± 0.04
	55	11.0 ± 1.0	10.9 ± 1.0	0.60 ± 0.03	0.40 ± 0.03
	60	24.0 ± 2.3	22.2 ± 2.3	1.22 ± 0.10	0.67 ± 0.07
Gl-PAI-1	37	0.062 ± 0.005	0.036 ± 0.003	0.008 ± 0.001	0.0006 ± 0.0001
	50	1.44 ± 0.10	0.43 ± 0.03	0.24 ± 0.03	0.077 ± 0.008
	55	2.16 ± 0.18	1.0 ± 0.11	0.50 ± 0.03	0.17 ± 0.02
	60	9.3 ± 1.1	4.9 ± 0.5	2.5 ± 0.3	0.63 ± 0.07

[a]Values of k_{L1}, k_{L2}, k_{L3}, and k_{L4} were determined from semilogarithmic plots of residual PAI-1 activity vs time (Figure 5) as described in Experimental Procedures.

interaction with tcuPA and tPA were studied to determine the association and dissociation rate constants (Scheme 1) and evaluate the effect of the ligands on the stoichiometry of inhibition for the reactions with target proteinases. A number of rPAI-1 mutant variants with a NBD group attached to a single cysteine at position P9 (reports RCL insertion[46]), P1′ (reports MC formation and movement of the primed part of the cleaved RCL[31]), or 119 (reports binding of Vn) were used to evaluate the kinetics of interaction of PAI-1 with S195A tcuPA and Vn (Scheme 1). The values of k_{+1}, k_{+2}, k_{+3}, and k_{+4} (Scheme 1) were determined using stopped-flow fluorimetry as previously described[26,41−42] from the slopes of the linear dependences of k_{obs} on the concentration of ligand (Figure 2 and Table 1). Diffusion-limited k_{+1} and k_{+4} [4.0−8.0 μM^{-1} s^{-1} (Figure 2 and Table 1)] were determined measuring the time traces of changes in fluorescence emission (excitation at 490 nm) of NBD P9, NBD P1′, and NBD S119C PAI-1 (k_{+1}) or their complexes with Vn (k_{+4}), due to the interaction with S195A tcuPA. Values of k_{+2} and k_{+3} [7.5 and 13.3 μM^{-1} s^{-1}, respectively (Figure 2 and Table 1)] were determined in a similar manner using NBD S119C PAI-1 (free or complexed with S195A tcuPA) and Vn. The second-order rate constants for interaction of S195A tcuPA with PAI-1 and PAI-1/Vn [k_{+1} and k_{+4}, respectively (Table 1)] were almost an order of magnitude lower than the association rate constant (k_{on} = 27 ± 1 μM^{-1} s^{-1}) for the interaction between S195A tPA and NBD P9 PAI-1.[31] However, when the contribution of ionic exosite interactions is minimized (0.5 M Hepes), the value of k_{on} (4.5 ± 0.1 μM^{-1} s^{-1})[31] becomes comparable to those for S195A tcuPA (Table 1). These results support the hypothesis of weaker exosite interactions between PAI-1 and uPA than between PAI-1 and tPA[47] and demonstrate that binding of Vn does not significantly change the second-order rate constant for interaction between PAI-1 and S195A tcuPA.

S195A tcuPA when bound to PAI-1 in a binary complex or in MSC (Figure 1) occupies the proteinase docking site (Scheme 1). Thus, neither of the two complexes is able to interact directly with the target proteinases. As a result, the dissociation of S195A tcuPA from PAI-1 or PAI-1/Vn [k_{-1} or k_{-4}, respectively (Scheme 1)] limits the rate of the reaction with tcuPA or tPA. NBD P9 PAI-1, which reports the insertion of the RCL into central β-sheet A due to the reaction with proteinase (Scheme 1) by a 6-fold increase in the fluorescence emission of the NBD group[46] and is biochemically similar to wt PAI-1,[35,31,46−,48] was used to determine rates of dissociation of S195A tcuPA. As expected (Figure 2), the observed rate constants (k_{obs}) for the reaction of the S195A tcuPA/NBD P9 PAI-1 complex or the corresponding MSC with tcuPA or tPA were independent of enzyme concentration [k_{-1} = (6.0 ± 0.3) × 10^{-3}, and k_{-4} = (4.0 ± 0.2) × 10^{-3} s^{-1} (Table 1, Scheme 1, and Figure 2)]. The values of k_{obs} for the inhibition of tPA and tcuPA with complexes of S195A tcuPA and rPAI-1, Gl-PAI-1, or Q123K PAI-1 (with or without Vn), which were measured in the presence of a fluorogenic substrate,[29] were also low [3.0−7.0 × 10^{-3} s^{-1} (Table 1)] and independent of enzyme concentration. Similar values of K_D, k_{-1}, and k_{-4} (Table 1) observed for different mutant variants of PAI-1 (with an exception of NBD P1′ PAI-1) indicate similar mechanisms driving the formation of MSCs. Therefore, high-affinity binding of S195A tcuPA and Vn to PAI-1, which is determined by the diffusion-limited (>1 μM^{-1} s^{-1}) association rate constants and slow (<10^{-2} s^{-1}) dissociation rate constants (Figure 2 and Table 1), governs the stabilization of the MSC. Binding of Vn, S195A tcuPA, or both ligands did not significantly affect the stoichiometry of inhibition for the reactions of every PAI-1 variant studied with either tPA or tcuPA (data not shown). Thus, active PAI-1 in a MSC (Figure 1) retains 100% capacity to inhibit equimolar amounts of target proteinase. However, in contrast to reactions of PAI-1 or PAI-1/Vn with target proteinases (Scheme 1), the rate of the reaction is limited by slow dissociation of S195A tcuPA.

The positively charged 37-loop of uPA or tPA could form exosite interactions with E350E351 (P4′P5′ nomenclature of Schechter and Berger[49]) of the RCL in PAI-1[35,50,51] and, thus, stabilize the MSC. To determine the contribution of P4′P5′ (Figure 1) to the stabilization of MSCs, k_{-1} and k_{-4} (Scheme 1) for complexes of S195A tcuPA with P4′P5′/AA NBD P9 PAI-1 were determined. The values of k_{-1} and k_{-4} [(7.0 ± 0.2) and (4.0 ± 0.2) × 10^{-3} s^{-1}, respectively (Table 1)] were similar to those observed for wt NBD P9 PAI-1 (Table 1). Therefore, the contribution of E350 and E351 to dissociation of the MSC or binary complex [k_{-4} and k_{-1}, respectively (Scheme 1)] is rather insignificant. This conclusion supports the molecular model of the S195A tcuPA/PAI-1 complex (Figure 1) that predicts that no direct interactions between the 37-loop of uPA and P4′P5′ occur (Figure 1).[32] In contrast to P4′P5′, the P1′ residue of the

dx.doi.org/10.1021/bi400470s | Biochemistry 2013, 52, 4697−4709

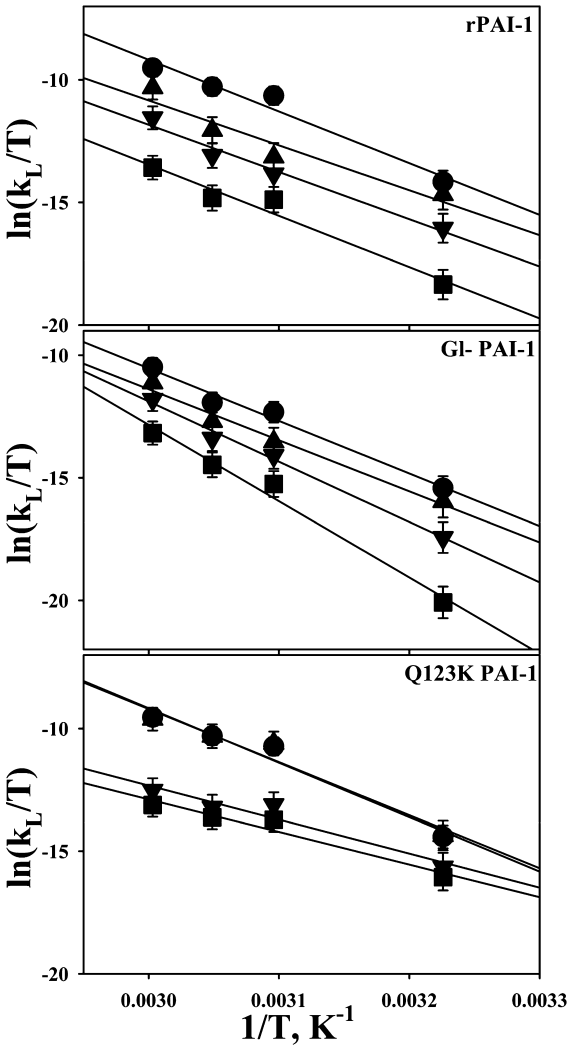

Figure 6. Eyring Plots for the spontaneous inactivation of PAI-1 alone (●) and PAI-1 in the presence of Vn (▲), S195A tcuPA (▼), and both ligands (■). Corresponding k_L values have been determined at 37, 50, 55, and 60 °C as described in Experimental Procedures (Table 2). Solid lines represent the best fit of the linear equation to the data. Values of the activation enthalpy ($\Delta H^{\ddagger}$) and entropy ($\Delta S^{\ddagger}$) (Table 3) were determined as −(slope) × R and [intercept − ln(k_B/h)] × R, where R, k_B, and h are 8.3145 J/mol, 1.3806×10^{-23} J/K, and 6.626×10^{-34} J/s, respectively.

RCL contributes to the stabilization of a MSC. The introduction of an NBD-labeled cysteine at the P1′ position (NBD P1′ PAI-1) resulted in increases in both k_{-1} and k_{-4} of 22.5- and 25-fold, respectively, without significant changes in k_{+1} and k_{+4} compared to those of NBD P9 PAI-1 (Table 1). To test whether exosite interactions other than P4′P5′ participate in the interaction between S195A tcuPA and PAI-1, the kinetics of the reaction between NBD P1′ PAI-1 and tcuPA were studied using stopped-flow fluorimetry (Figure 3) and compared to that for NBD P9 PAI-1.[26,41,31] Similar to the reaction between NBD P1′ PAI-1 and tPA,[31] biphasic changes in NBD fluorescence emission were observed for the reaction between NBD P1′ PAI-1 and tcuPA (Figure 3, inset) and reflect the fast formation of a noncovalent transient intermediate complex between PAI-1 and the enzyme followed by dissociation of the primed end of the cleaved RCL. In contrast to trypsin and similar to tPA,[31] an increase in the K_D for NBD P1′ PAI-1, when compared to that of NBD P9 PAI-1 (Table 1), paralleled an increase in the corresponding K_M (Scheme 2) from 2.8 ± 0.6 to 10.0 ± 4.0 μM (Figure 3). Therefore, while P4′P5′ do not stabilize the MSC, other exosite interactions, which are perturbed by a mutation at P1′, likely contribute to the binding of tcuPA to PAI-1 and to the stabilization of the MSC (Figure 1).

MSC Slows the Spontaneous Inactivation of PAI-1 by 2 Orders of Magnitude. Under k_{lim} = 0 conditions (Scheme 1), which are characteristic of both MC and MSC (Scheme 1) formed with S195A tcuPA, the spontaneous insertion of uncleaved RCL into β-sheet A due to the active to latent transition [k_{L1}, k_{L2}, k_{L3}, and k_{L4} (Scheme 1)] becomes the major mechanism of inactivation of PAI-1. Individually, Vn and S195A tcuPA stabilize the active conformation of PAI-1.[2,4] On the basis of the additivity of effects of mAbs and Vn on the PAI-1 mechanism observed previously,[26,27,41] we hypothesized that both ligands (Figure 1) affect the stability of the active PAI-1 conformation additively or even synergistically. To compare the effects of S195A tcuPA, Vn, and both ligands on the rate of the spontaneous active to latent transition of PAI-1 (Scheme 1) under physiological conditions, wt rPAI-1 and Gl-PAI-1 were incubated with one or both ligands in 0.02 M Hepes and 0.13 M NaCl (pH 7.4) at 37 °C. In the control experiments, Gl-PAI-1 and rPAI-1 were incubated without ligands under the same conditions. Q123K PAI-1 (lacks ability to bind Vn[45]) was used to evaluate the contribution of possible nonspecific interactions with Vn. Aliquots were withdrawn at 0, 1, 15, 90, and 720 h and incubated with excess sctPA for 0.5−1.0 h at 37 °C followed by SDS−PAGE analysis (Figure 4A). Active PAI-1 was visualized as SIC with tPA either by staining with SYPRO Ruby protein (0−90 h) or by Western blot analysis for the PAI-1 antigen (720 h).

While at time points 0 and 1 h (Figure 4A) active PAI-1 was observed in every reaction mixture, only two (rPAI-1 and Gl-PAI-1 incubated with both Vn and S195A tcuPA) contained active serpin at 90 and 720 h (Figure 4A). Notably, active conformations of rPAI-1 and Gl-PAI-1 were detected by two independent methods: Western blotting (Figure 4A, bottom panel) and inhibition of activation of human Glu-plasminogen (Plg) by tcuPA (Figure 4B) after 1 month (720 h) at 37 °C. Therefore, S195A tcuPA and Vn slow spontaneous PAI-1 inactivation at 37 °C by almost 2 orders of magnitude and do not significantly affect the stoichiometry of inhibition for tPA (Figure 4A) or uPA (Figure 4). Because the stoichiometry of inhibition for the reaction between MSCs and target proteinases remains close to unity, PAI-1 in MSCs retains the ability to inactivate almost equimolar amounts of tPA or uPA significantly longer than free serpin or its complex with Vn (Scheme 1). While normal levels of endogenous PAI-1 in plasma are relatively low (6−80 ng/mL[52,53]), its concentration is elevated by up to 3 orders of magnitude in a number of pathological conditions.[54,55] Thus, accumulation of endogenous active PAI-1 in MSCs could result in the inefficiency of S195A proteinase variants (and similar inhibitors, which compete with target proteinases for active PAI-1) for neutralizing PAI-1 *in vivo*. Formation of MSCs protects endogenous PAI-1/Vn [low k_{L4}/k_{L2} (Figure 4 and Scheme 1)] from inactivation by preventing the spontaneous transition from the active to latent form. Thus, accumulation of PAI-1, stabilized in the active conformation by MSCs, could result in an increased capacity to inactivate higher levels of target proteinases.

dx.doi.org/10.1021/bi400470s | *Biochemistry* 2013, 52, 4697−4709

Table 3. Activation Enthalpies ($\Delta H^{\ddagger}$), Entropies ($\Delta S^{\ddagger}$), and Gibbs Free Activation Energies ($\Delta G^{\ddagger}$) for the Spontaneous Active to Latent Transition for wt rPAI-1, Q123K PAI-1, and wt Gl-PAI-1 and Their Complexes with Vn, S195A tcuPA, and Both Ligands at 37 °C

	ligand				
serpin	S195A tcuPA	Vn	$\Delta H^{\ddagger a}$ (kJ/mol)	$\Delta S^{\ddagger b}$ (J mol^{-1} K^{-1})	$\Delta G^{\ddagger c}$ (kJ/mol)
rPAI-1	−	−	175.3 ± 12.8	255.5 ± 16.7	96.1
Q123K PAI-1	−	−	184.5 ± 14.2	283.2 ± 19.7	96.7
Gl-PAI-1	−	−	178.3 ± 11.4	253.3 ± 18.3	99.8
rPAI-1	−	+	152.4 ± 9.6	173.0 ± 14.0	98.7
Q123K PAI-1	−	+	179.9 ± 11.0	269.1 ± 17.3	96.4
Gl-PAI-1	−	+	173.1 ± 12.7	230.8 ± 15.7	101.6
rPAI-1	+	−	160.1 ± 9.8	188 ± 13.3	101.8
Q123K PAI-1	+	−	115.2 ± 8.4	49.2 ± 4.7	100.0
Gl-PAI-1	+	−	204.3 ± 16.6	320.2 ± 24.7	105.1
rPAI-1	+	+	173.8 ± 10.6	215.4 ± 16.7	107.0
Q123K PAI-1	+	+	110.5 ± 9.4	30.5 ± 2.7	101.1
Gl-PAI-1	+	+	258.5 ± 16.7	474.6 ± 25.6	111.3

[a]Values of activation enthalpy $\Delta H^{\ddagger}$ were calculated from linear ($r^2 > 0.9$) Eyring plots (Figure 6) as −(slope) × 8.3145 J/mol. [b]Values of activation entropy $\Delta S^{\ddagger}$ were calculated from Eyring plots (Figure 6) as (intercept − 23.76) × 8.3145 J mol^{-1} K^{-1}. [c]Values of $\Delta G^{\ddagger}$ at 37 °C were calculated as $\Delta G^{\ddagger} = \Delta H^{\ddagger} - T\Delta S^{\ddagger}$.

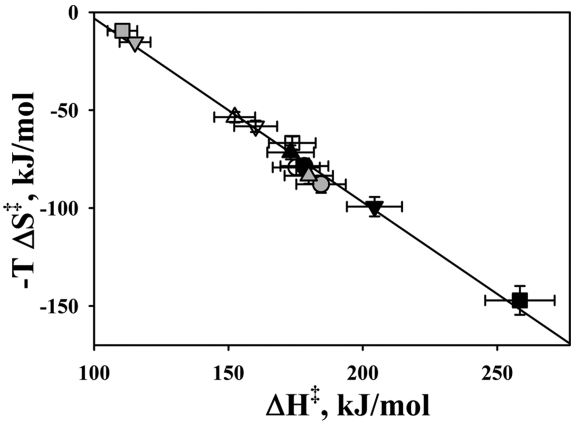

Figure 7. Enthalpy−entropy compensation. A linear correlation between changes in the contribution of $-T\Delta S^{\ddagger}$ and $\Delta H^{\ddagger}$ (Table 3) to $\Delta G^{\ddagger}$ for the three PAI-1 variants and their complexes with ligands at 37 °C. The values of $-T\Delta S^{\ddagger}$ for rPAI-1 (white symbols), Gl-PAI-1 (black symbols), and Q123K PAI-1 (gray symbols) for free serpins (circles) and their complexes with Vn (triangles), S195A tcuPA (inverted triangles), and both ligands (squares) were plotted as a function of $\Delta H^{\ddagger}$. The solid line represents the best fit of the linear equation $-T\Delta S^{\ddagger} = 90.6 - 0.94\Delta H^{\ddagger}$ ($r^2 = 0.99$) to the data.

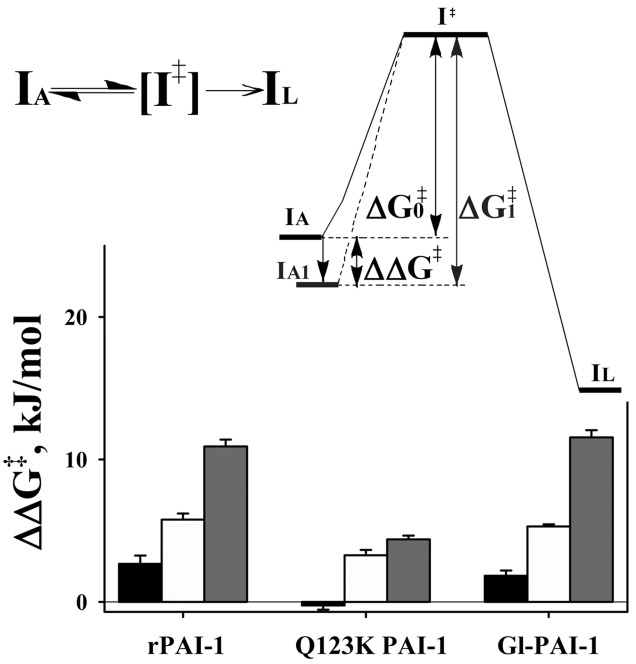

Figure 8. Synergistic stabilization of the active conformation of PAI-1 in MSC. Scheme 3 shows a transition intermediate ($I^{\ddagger}$), which is in equilibrium with active PAI-1 (I_A), forms during conformational changes accompanying the transition to the latent conformation (I_L).[43] A diagram depicts how I_A is stabilized in the complex with ligand(s) (I_{A1}) because of an increase in $\Delta G^{\ddagger}$ ($\Delta\Delta G^{\ddagger} = \Delta G^{\ddagger}_1 - \Delta G^{\ddagger}_0$), where $\Delta G^{\ddagger}_1$ and $\Delta G^{\ddagger}_0$ are changes in the activation Gibbs free energy for active PAI-1 with and without ligand(s), respectively. A bar graph shows the contribution of Vn (black), S195A tcuPA (white), and both ligands (gray) to $\Delta\Delta G^{\ddagger}$ for rPAI-1, Q123K PAI-1, and Gl-PAI-1 at 37 °C. The values of $\Delta G^{\ddagger}_0$ and $\Delta G^{\ddagger}_1$ were calculated as $\Delta G^{\ddagger} = \Delta H^{\ddagger} - T\Delta S^{\ddagger}$ (Table 3).

Thermodynamics of Stabilization of PAI-1 in a MSC. To evaluate the forces governing the stabilization of the active conformation of PAI-1, rates of spontaneous inactivation of free rPAI-1, Gl-PAI-1, and Q123K PAI-1 and their complexes with one or both ligands were determined at 37, 50, 55, and 60 °C for free serpins. PAI-1 activity was determined in the aliquots withdrawn at different time points by titration with sctPA as previously described.[9] The first-order rate constants [k_{L1}, k_{L2}, k_{L3}, and k_{L4} (Scheme 1)] for rPAI-1, Gl-PAI-1, and Q123K PAI-1 in the presence of S195A tcuPA, Vn, and both ligands were estimated from the slopes of linear dependences of semilogarithmic plots of residual PAI-1 activity versus time (Figure 5). The values of k_{L1}, k_{L2}, k_{L3}, and k_{L4} were determined by titrating the residual active PAI-1 (Figure 5, filled symbols) present in aliquots withdrawn at different time points with increasing amounts of sctPA. Rate constants at 50 °C (Figure 5, empty symbols) and at 37 °C (not shown) were also estimated from the results of SDS−PAGE. The $k_{L1}^{SDS-PAGE}$, $k_{L2}^{SDS-PAGE}$, $k_{L3}^{SDS-PAGE}$, and $k_{L4}^{SDS-PAGE}$ were assessed from changes in PAI-1 activity with time, determined by densitometry of digitized images from SDS−PAGE (Figure 5, empty symbols). Active PAI-1, which formed SIC, was estimated as a fraction of total PAI-1 (latent, cleaved, and complexed with sctPA). While

dx.doi.org/10.1021/bi400470s | Biochemistry 2013, 52, 4697−4709

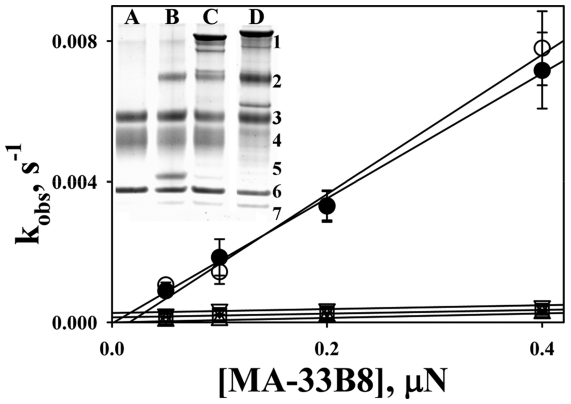

Figure 9. MSCs formed with S195A tcuPA and mAbs protect rPAI-1/Vn from inactivation by MA-33B8 and the spontaneous active to latent transition. Dependences of k_{obs} for RCL insertion for NBD P9 PAI-1 (●), NBD P9 PAI-1/Vn (○), and MSCs with MA-56A7C10 (△), MA-44E4 (□), and S195A tcuPA (▽) on MA-33B8 concentration. NBD P9 PAI-1, its complex with Vn (10 nM), and MSCs formed in the presence of 20 nM S195A tcuPA or a mAb (MA-56A7C10 or MA-44E4) were incubated with MA-33B8 (50−400 nN) in 96-well flat bottom plates from Costar (Corning Inc.), and an increase in NBD fluorescence with time was registered using a fluorescence spectrophotometer SynergyTM HT Hybrid Reader. The k_{obs} values were calculated by fitting a single-exponential equation to the data using Gen5 version 2.0 (BioTek) and SigmaPlot version 11.0 (SPSS Inc.), as described previously.[26,41,42] The inset shows the stabilization of rPAI-1/Vn (lane A) in MSCs with S195A tcuPA (lane B), MA-56A7C10 (lane C), and MA-42A2F6 (lane D) after incubation at 37 °C for 168 h (1 week). Active PAI-1 was quenched by sctPA, and reaction mixtures were analyzed as described in Experimental Procedures. Positions of mAb (1), PAI-1/tPA SIC (2), Vn (3), tPA (4), S195A tcuPA (5), latent PAI-1 (6), and cleaved PAI-1 (7) are indicated to the right of the gel.

the measurements of amidolytic tPA activity are more accurate, only SDS−PAGE analysis provides direct proof (formed SIC) of active PAI-1 in the aliquot. Both sets of rate constants (Figure 5, inset) correlated with each other for all three PAI-1 variants studied. A decrease in k_L (k_{L1}/k_{L4}) at 50 °C due to MSC formation approaches 2 orders of magnitude for Gl-PAI-1 and rPAI-1 (Figure 5, inset). The values of k_{L1}, k_{L2}, k_{L3}, and k_{L4} for the temperatures studied are listed in Table 2.

To determine effects of Vn, S195A tcuPA, and both ligands on changes in the activation enthalpy ($\Delta H^{\ddagger}$), entropy ($\Delta S^{\ddagger}$), and Gibbs free energy ($\Delta G^{\ddagger}$) for the reaction of spontaneous inactivation of rPAI-1, Gl-PAI-1, and Q123K PAI-1, Eyring plots (Figure 6) were analyzed. The values of $\Delta H^{\ddagger}$ and $\Delta S^{\ddagger}$ (Table 3) were determined from linear Eyring plots (Figure 6). The enthalpy−entropy compensation plot (Figure 7) illustrates the difference in the effects of Vn, S195A tcuPA, and both ligands together on the contribution of $\Delta H^{\ddagger}$ and $-T\Delta S^{\ddagger}$ to $\Delta G^{\ddagger}$ at 37 °C. A positive $\Delta H^{\ddagger}$ controls the stability of active PAI-1, and because of a positive $\Delta S^{\ddagger}$, increasing the temperature results in an increase in the rate of the spontaneous active to latent transition (Table 3). Vn induces a decrease in $\Delta S^{\ddagger}$, which governs the stabilization of both rPAI-1 and Gl-PAI-1 (Figure 7 and Table 3). Stabilization of rPAI-1 and Q123K PAI-1 by S195A tcuPA (with or without Vn) is driven by a decrease in $\Delta S^{\ddagger}$. In contrast, Gl-PAI-1 is stabilized because of a significant increase in $\Delta H^{\ddagger}$ (Figure 7 and Table 3). Such an increase in $\Delta H^{\ddagger}$ could indicate the formation of additional exosite interactions between S195A tcuPA and Gl-PAI-1 that further stabilize the exposed RCL.

The simplest mechanism of the transition from the active (I_A) to latent (I_L) conformation of PAI-1 (Figure 8 and Scheme 3 therein) includes a transient intermediate ($I^{\ddagger}$), which exists in equilibrium with active PAI-1.[43] While moving the equilibrium toward the formation of $I^{\ddagger}$ results in an increase in the rate of spontaneous inactivation of PAI-1,[43] a decrease in the level of $I^{\ddagger}$ should suppress the active to latent transition. Comparing the changes in the Gibbs free energy of activation [$\Delta\Delta G^{\ddagger} = \Delta G^{\ddagger}_0 - \Delta G^{\ddagger}_1$, where $\Delta G^{\ddagger}_0$ and $\Delta G^{\ddagger}_1$ correspond to free PAI-1 and its complex with the ligand(s), respectively (Figure 8 and Scheme 3)] allows determination of the contribution of Vn, S195A tcuPA, and both ligands together to the stabilization of the active conformation of PAI-1 variants. An increase in $\Delta\Delta G^{\ddagger}$ (Scheme 3) in the presence of both Vn and S195A tcuPA equal to or greater than the sum of the effects of each ligand indicates additive or synergistic stabilization of I_A, respectively. Values of $\Delta\Delta G^{\ddagger}$ induced by Vn ($\Delta\Delta G^{\ddagger}_{Vn}$), S195A tcuPA ($\Delta\Delta G^{\ddagger}_{S195A\ tcuPA}$), and both ligands ($\Delta\Delta G^{\ddagger}_{Vn/S195A\ tcuPA}$) at 37 °C are shown in Figure 8 for the three variants of PAI-1 studied. Notably, $\Delta\Delta G^{\ddagger}_{Vn/S195A\ tcuPA}$ values were similar for both wild-type variants, rPAI-1 and Gl-PAI-1 (Figure 8). Moreover, because the increase in $\Delta G^{\ddagger}$ caused by the binding of both ligands ($\Delta\Delta G^{\ddagger}_{Vn/S195A\ tcuPA}$) was greater (by 4.4 and 2.6 kJ/mol for Gl-PAI-1 and rPAI-1, respectively) than $\Delta\Delta G^{\ddagger}_{Vn} + \Delta\Delta G^{\ddagger}_{S195A\ tcuPA}$ (Figure 8 and Table 3), Vn and S195A tcuPA act synergistically. Under experimental conditions used in this study, Vn did not stabilize Q123K PAI-1 and its $\Delta\Delta G^{\ddagger}_{Vn/S195A\ tcuPA}$ was significantly lower than that for wt PAI-1 (Figure 8). However, some increase in $\Delta\Delta G^{\ddagger}_{Vn/S195A\ tcuPA}$ over $\Delta\Delta G^{\ddagger}_{S195A\ tcuPA}$ observed for Q123K PAI-1 (Figure 8 and Table 3) could reflect the effects of nonspecific binding of Vn. The synergistic effect of S195A tcuPA and Vn on the stability of PAI-1 [$\Delta\Delta G^{\ddagger}_{Vn/S195A\ tcuPA} > \Delta\Delta G^{\ddagger}_{Vn} + \Delta\Delta G^{\ddagger}_{S195A\ tcuPA}$ (Figure 8)] could originate from enhanced stabilization of the exposed RCL by S195A tcuPA bound to a less flexible PAI-1 molecule[20] and reflect a shift of the position of the equilibrium (Figure 8 and Scheme 3[43]) from a transient prelatent intermediate $I^{\ddagger}$ toward I_A (Scheme 3). A disruption of the binding of either of the two ligands results in a dramatic decrease in the stability of the active conformation of PAI-1 as observed with Q123K PAI-1 or both binary complexes (Figures 4 and 5).

Notably, the values of $\Delta G^{\ddagger}$ observed for wt rPAI-1 were always lower than those found for wt Gl-PAI-1 (Table 3). A higher $\Delta G^{\ddagger}$ reflects the higher stability of the glycosylated serpin (alone and in complexes with the ligands) and supports a recent report.[44] The differences in the stability between wt rPAI-1 and Gl-PAI-1 ($\Delta\Delta G^{\ddagger}_{Gl} = \Delta G^{\ddagger}_{Gl\text{-}PAI\text{-}1} - \Delta G^{\ddagger}_{rPAI\text{-}1}$) were 3.7, 2.9, 3.3, and 4.3 kJ/mol for free serpins and their complexes with Vn, S195A tcuPA, and both ligands, respectively (Table 3). Thus, $\Delta\Delta G^{\ddagger}_{Gl}$ likely reflects the contribution of glycosylation of the PAI-1 molecule to the stabilization of active PAI-1 and its complexes.

Anti-PAI-1 mAbs Form MSCs, Stabilize PAI-1/Vn, and Protect PAI-1 from Inactivation with MA-33B8. Anti-human PAI-1 mAb MA-33B8 significantly accelerates the spontaneous active to latent transition of PAI-1 and PAI-1/Vn [increases k_{L1} and k_{L2} (Scheme 1)] by binding with high affinity to both the prelatent intermediate and latent PAI-1 [$I^{\ddagger}$ and I_L, respectively (Scheme 3)].[43] To test whether active PAI-1 in MSCs is protected from inactivation, NBD P9 PAI-1, its

dx.doi.org/10.1021/bi400470s | Biochemistry 2013, 52, 4697−4709

complex with Vn, and its complex with both ligands (Vn and S195A tcuPA) were incubated with different amounts of MA-33B8, and the rate of the active to latent transition was determined as previously described.[43] The k_{obs} of RCL insertion was increased linearly with MA-33B8 concentration for NBD P9 PAI-1 and its complex with Vn (Figure 9).[43] In contrast, the k_{obs} for MSCs was much lower and independent of the MA-33B8 concentration (Figure 9). Because the epitope of MA-33B8 does not overlap with the proteinase docking site,[56] formation of a MSC likely restricts the movements of the RCL in the active PAI-1 and thus decreases the concentration of $I^{\ddagger}$ by shifting the equilibrium (Scheme 3) toward the active conformation of PAI-1 (I_A).

To determine whether ligands other than proteinase could form MSCs with PAI-1/Vn and affect the rate of its spontaneous inactivation, anti-PAI-1 mAbs (MA-56A7C10, MA-42A2F6, and MA-44E4) that compete with proteinase[34] were tested. These mAbs interact with the PAI-1 with nanomolar affinity at epitopes close to the proteinase docking site[34] and form a MSC with PAI-1/Vn [$k_{lim2} = 0$ (Scheme 1)], substituting for S195A tcuPA (Figure 1). Similar to S195A tcuPA, MA-56A7C10, MA-44E4 (Figure 9), and MA-42A2F6 (not shown) effectively protected NBD P9 PAI-1/Vn from inactivation with MA-33B8. Therefore, it is likely that anti-PAI-1 mAbs that compete for PAI-1 with target proteinases and S195A tcuPA affect the reaction between PAI-1/Vn and MA-33B8 via the same mechanism.

To compare the effects of MSCs formed with S195A tcuPA and anti-PAI-1 mAbs on the rate of the active to latent transition, MA-56A7C10, MA-42A2F6 (Figure 9, inset), and MA-44E4 (not shown) were incubated with PAI-1/Vn at 37 °C for 168 h and analyzed for the presence of PAI-1 in the active conformation, using SDS−PAGE (Figure 9, inset). Similar to S195A tcuPA, all three anti-PAI-1 mAbs had k_{-1} and k_{-4} values in the range of 10^{-4} to 10^{-3} s^{-1} (not shown), formed MSCs, and stabilized active PAI-1 (Figure 9, inset). These results demonstrate that MSCs, which stabilize active PAI-1 by moving the equilibrium toward I_A (Figure 8 and Scheme 3), are resistant to MA-33B8-type PAI-1 inhibitors.

Stabilization of endogenous PAI-1/Vn in MSCs is a novel mechanism that can generate durable antiproteinase activity. If operative *in vivo*, these complexes have the potential to create and promote fibrin deposition and profibrotic repair. Because of a stoichiometry of inhibition close to unity, MSCs are able to inactivate close to equimolar amounts of target proteinases. Active PAI-1 is a molecular target in fibrinolytic therapy[2,9] and cancer,[57] and its neutralization improves outcomes in animal models.[9,58,59] Thus, the possibility of MSC formation *in vivo* should be considered if S195A inactive proteinases or mAbs competing for PAI-1 are used. The effects of MSCs on PAI-1 specificity and signaling cascades, as well as MSC metabolism and mechanisms of clearance, have yet to be investigated. In addition, the relative effects of increasing the thermodynamic stability of PAI-1 (to a half-life of days) versus its normal clearance rate (a half-life of ∼30 min) will need to be evaluated as an important factor that could affect PAI-1 activity. Nevertheless, redirection of the PAI-1 mechanism toward the substrate pathway by mAbs[26,28,41] or by low-molecular weight inhibitors[59] could be used to neutralize MSCs.

While, to the best of our knowledge, there are no reports of endogenous MSCs, a significant increase in the level of active PAI-1 was reported in a number of severe pathologies.[60,61] An increase of more than 2 orders of magnitude in the concentration of PAI-1 in sepsis, complicated parapneumonics, and empyema is accompanied by an increase in both PAI-1 activity and the fraction of the active PAI-1 present in the circulation or pleural fluids.[60,61] Moreover, a 1.5−2.5-fold increase in PAI-1 activity without changes in the total antigen was observed between days 1 and 3 in severe pediatric sepsis.[61] While such an accumulation of the active PAI-1 could indicate its stabilization or/and slower clearance, this increase in PAI-1 activity has been strongly correlated with unresolved multiple-organ failure and a lethal outcome.[61] Recently, the mechanisms of PAI-1 overexpression were studied in an animal model of microbial sepsis that recapitulates human disease[62] and thus could provide a rationale for further evaluation of PAI-1 as a prognostic factor[63−66] and possible target in severe sepsis and disseminated intravascular coagulation.

AUTHOR INFORMATION

Corresponding Author

*The University of Texas Health Science Center at Tyler (UTHSCT), 11937 U.S. Highway 271, Tyler, TX 75708. E-mail: andrey.komissarov@uthct.edu. Phone: (903) 877-5183. Fax: (903) 877-5627.

Funding

This work was supported by National Heart, Lung and Blood Institute Grant P50 HL107186-02 and the Texas Lung Injury Institute.

Notes

The authors declare no competing financial interest.

ACKNOWLEDGMENTS

We thank Genentech Inc. for providing sctPA.

ABBREVIATIONS

Gl, glycosylated; mAb, monoclonal antibody; MC, Michaelis complex; MSC, molecular sandwich complex; NBD, *N*-{[2-(iodoacetoxy)ethyl]-*N*-methyl}amino-7-nitrobenz-2-oxa-3-diazole; NBD P1′ PAI-1, Met447Cys PAI-1 with the NBD group attached to the cysteine; NBD P9 PAI-1, Ser338Cys PAI-1 with the NBD group attached to the cysteine; NBD S119C PAI-1, Ser119Cys PAI-1 with the NBD group attached to the cysteine; Q123K PAI-1, nonglycosylated Gln123Lys vitronectin reduced binding PAI-1 mutant; P4′P5′/AA NBD P9 PAI-1, E350A/E351A double mutant of NBD P9 PAI-1; PAI-1, plasminogen activator inhibitor 1; Plg, human Glu-plasminogen; r, non-glycosylated; RCL, reactive center loop; S195A tcuPA, tcuPA with a Ser195Ala substitution (chymotrypsin numbering); sc, single-chain; SIC, stable inhibitory complex; SMB, somatomedin B domain of vitronectin; $t_{1/2}$, half-life; tc, two-chain; tPA, tissue-type plasminogen activator; uPA, urokinase; Vn, vitronectin; wt, wild type.

REFERENCES

(1) Iwaki, T., Urano, T., and Umemura, K. (2012) PAI-1, progress in understanding the clinical problem and its aetiology. *Br. J. Haematol. 157*, 291−298.

(2) Van De Craen, B., Declerck, P. J., and Gils, A. (2012) The biochemistry, physiology and pathological roles of PAI-1 and the requirements for PAI-1 inhibition in vivo. *Thromb. Res. 130*, 576−585.

(3) Czekay, R. P., Wilkins-Port, C. E., Higgins, S. P., Freytag, J., Overstreet, J. M., Klein, R. M., Higgins, C. E., Samarakoon, R., and Higgins, P. J. (2011) PAI-1: An Integrator of Cell Signaling and Migration. *Int. J. Cell Biol. 2011*, 562481.

(4) Declerck, P. J., and Gils, A. (2013) Three Decades of Research on Plasminogen Activator Inhibitor-1: A Multifaceted Serpin. *Semin. Thromb. Hemostasis 39*, 356−364.
(5) Gando, S., Nakanishi, Y., and Tedo, I. (1995) Cytokines and plasminogen activator inhibitor-1 in posttrauma disseminated intravascular coagulation: Relationship to multiple organ dysfunction syndrome. *Crit. Care Med. 23*, 1835−1842.
(6) Iba, T., Kidokoro, A., Fukunaga, M., Sugiyama, K., Sawada, T., and Kato, H. (2005) Association between the severity of sepsis and the changes in hemostatic molecular markers and vascular endothelial damage markers. *Shock 23*, 25−29.
(7) Idell, S., Girard, W., Koenig, K. B., McLarty, J., and Fair, D. S. (1991) Abnormalities of pathways of fibrin turnover in the human pleural space. *Am. Rev. Respir. Dis. 144*, 187−194.
(8) Semeraro, N., Ammollo, C. T., Semeraro, F., and Colucci, M. (2012) Sepsis, thrombosis and organ dysfunction. *Thromb. Res. 129*, 290−295.
(9) Karandashova, S., Florova, G., Azghani, A. O., Komissarov, A. A., Koenig, K., Tucker, T. A., Allen, T. C., Stewart, K., Tvinnereim, A., and Idell, S. (2013) Intrapleural adenoviral delivery of human plasminogen activator inhibitor-1 exacerbates tetracycline-induced pleural injury in rabbits. *Am. J. Respir. Cell Mol. Biol. 48*, 44−52.
(10) Balsara, R. D., Xu, Z., and Ploplis, V. A. (2007) Targeting plasminogen activator inhibitor-1: Role in cell signaling and the biology of domain-specific knock-in mice. *Curr. Drug Targets 8*, 982−995.
(11) Chaillan-Huntington, C. E., Gettins, P. G. W., Huntington, J. A., and Patston, P. A. (1997) The P6-P2 region of serpins is critical for proteinase inhibition and complex stability. *Biochemistry 36*, 9562−9570.
(12) Kruithof, E. K. (1988) Plasminogen activator inhibitors: A review. *Enzyme 40*, 113−121.
(13) Wiman, B., Almquist, A., Sigurdardottir, O., and Lindahl, T. (1988) Plasminogen activator inhibitor 1 (PAI) is bound to vitronectin in plasma. *FEBS Lett. 242*, 125−128.
(14) Tomasini, B. R., and Mosher, D. F. (1991) Vitronectin. *Prog. Hemostasis Thromb. 10*, 269−305.
(15) Preissner, K. T., and Seiffert, D. (1998) Role of vitronectin and its receptors in haemostasis and vascular remodeling. *Thromb. Res. 89*, 1−21.
(16) Declerck, P. J., De Mol, M., Alessi, M. C., Baudner, S., Paques, E. P., Preissner, K. T., Muller-Berghaus, G., and Collen, D. (1988) Purification and characterization of a plasminogen activator inhibitor 1 binding protein from human plasma. Identification as a multimeric form of S protein (vitronectin). *J. Biol. Chem. 263*, 15454−15461.
(17) Preissner, K. T., Grulich-Henn, J., Ehrlich, H. J., Declerck, P., Justus, C., Collen, D., Pannekoek, H., and Muller-Berghaus, G. (1990) Structural requirements for the extracellular interaction of plasminogen activator inhibitor 1 with endothelial cell matrix-associated vitronectin. *J. Biol. Chem. 265*, 18490−18498.
(18) van Meijer, M., Gebbink, R. K., Preissner, K. T., and Pannekoek, H. (1994) Determination of the vitronectin binding site on plasminogen activator inhibitor 1 (PAI-1). *FEBS Lett. 352*, 342−346.
(19) Fa, M., Karolin, J., Aleshkov, S., Strandberg, L., Johansson, L. B., and Ny, T. (1995) Time-resolved polarized fluorescence spectroscopy studies of plasminogen activator inhibitor type 1: Conformational changes of the reactive center upon interactions with target proteases, vitronectin and heparin. *Biochemistry 34*, 13833−13840.
(20) Trelle, M. B., Hirschberg, D., Jansson, A., Ploug, M., Roepstorff, P., Andreasen, P. A., and Jorgensen, T. J. (2012) Hydrogen/Deuterium Exchange Mass Spectrometry Reveals Specific Changes in the Local Flexibility of Plasminogen Activator Inhibitor 1 upon Binding to the Somatomedin B Domain of Vitronectin. *Biochemistry 51*, 8256−8266.
(21) Ehrlich, H. J., Gebbink, R. K., Keijer, J., Linders, M., Preissner, K. T., and Pannekoek, H. (1990) Alteration of serpin specificity by a protein cofactor. Vitronectin endows plasminogen activator inhibitor 1 with thrombin inhibitory properties. *J. Biol. Chem. 265*, 13029−13035.
(22) Ehrlich, H. J., Gebbink, R. K., Preissner, K. T., Keijer, J., Esmon, N. L., Mertens, K., and Pannekoek, H. (1991) Thrombin neutralizes plasminogen activator inhibitor 1 (PAI-1) that is complexed with vitronectin in the endothelial cell matrix. *J. Cell Biol. 115*, 1773−1781.
(23) Keijer, J., Ehrlich, H. J., Linders, M., Preissner, K. T., and Pannekoek, H. (1991) Vitronectin governs the interaction between plasminogen activator inhibitor 1 and tissue-type plasminogen activator. *J. Biol. Chem. 266*, 10700−10707.
(24) van Meijer, M., Stoop, A., Smilde, A., Preissner, K. T., van Zonneveld, A. J., and Pannekoek, H. (1997) The composition of complexes between plasminogen activator inhibitor 1, vitronectin and either thrombin or tissue-type plasminogen activator. *Thromb. Haemostasis 77*, 516−521.
(25) Rezaie, A. R. (2001) Vitronectin functions as a cofactor for rapid inhibition of activated protein C by plasminogen activator inhibitor-1. Implications for the mechanism of profibrinolytic action of activated protein C. *J. Biol. Chem. 276*, 15567−15570.
(26) Komissarov, A. A., Andreasen, P. A., Bodker, J. S., Declerck, P. J., Anagli, J. Y., and Shore, J. D. (2005) Additivity in effects of vitronectin and monoclonal antibodies against α-helix F of plasminogen activator inhibitor-1 on its reactions with target proteinases. *J. Biol. Chem. 280*, 1482−1489.
(27) Komissarov, A. A., Zhou, A., and Declerck, P. J. (2007) Modulation of serpin reaction through stabilization of transient intermediate by ligands bound to α-helix F. *J. Biol. Chem. 282*, 26306−26315.
(28) Komissarov, A. A., Andreasen, P. A., Declerck, P. J., Kamikubo, Y., Zhou, A., and Gruber, A. (2008) Redirection of the reaction between activated protein C and a serpin to the substrate pathway. *Thromb. Res. 122*, 397−404.
(29) Sen, P., Komissarov, A. A., Florova, G., Idell, S., Pendurthi, U. R., and Vijaya Mohan, R. L. (2011) Plasminogen activator inhibitor-1 inhibits factor VIIa bound to tissue factor. *J. Thromb. Haemostasis 9*, 531−539.
(30) Bartha, K., Declerck, P. J., Moreau, H., Nelles, L., and Collen, D. (1991) Synthesis and secretion of plasminogen activator inhibitor 1 by human endothelial cells in vitro. Effect of active site mutagenized tissue-type plasminogen activator. *J. Biol. Chem. 266*, 792−797.
(31) Olson, S. T., Swanson, R., Day, D., Verhamme, I., Kvassman, J., and Shore, J. D. (2001) Resolution of Michaelis complex, acylation, and conformational change steps in the reactions of the serpin, plasminogen activator inhibitor-1, with tissue plasminogen activator and trypsin. *Biochemistry 40*, 11742−11756.
(32) Lin, Z., Jiang, L., Yuan, C., Jensen, J. K., Zhang, X., Luo, Z., Furie, B. C., Furie, B., Andreasen, P. A., and Huang, M. (2011) Structural basis for recognition of urokinase-type plasminogen activator by plasminogen activator inhibitor-1. *J. Biol. Chem. 286*, 7027−7032.
(33) Zhou, A., Huntington, J. A., Pannu, N. S., Carrell, R. W., and Read, R. J. (2003) How vitronectin binds PAI-1 to modulate fibrinolysis and cell migration. *Nat. Struct. Biol. 10*, 541−544.
(34) Bijnens, A. P., Gils, A., Stassen, J. M., Komissarov, A. A., Knockaert, I., Brouwers, E., Shore, J. D., and Declerck, P. J. (2001) The distal hinge of the reactive site loop and its proximity: A target to modulate plasminogen activator inhibitor-1 activity. *J. Biol. Chem. 276*, 44912−44918.
(35) Ibarra, C. A., Blouse, G. E., Christian, T. D., and Shore, J. D. (2004) The contribution of the exosite residues of plasminogen activator inhibitor-1 to proteinase inhibition. *J. Biol. Chem. 279*, 3643−3650.
(36) Idell, S., Mazar, A., Cines, D., Kuo, A., Parry, G., Gawlak, S., Juarez, J., Koenig, K., Azghani, A., Hadden, W., McLarty, J., and Miller, E. (2002) Single-chain urokinase alone or complexed to its receptor in tetracycline-induced pleuritis in rabbits. *Am. J. Respir. Crit. Care Med. 166*, 920−926.
(37) Komissarov, A. A., Mazar, A. P., Koenig, K., Kurdowska, A. K., and Idell, S. (2009) Regulation of intrapleural fibrinolysis by urokinase-α-macroglobulin complexes in tetracycline-induced pleural injury in rabbits. *Am. J. Physiol. 297*, L568−L577.
(38) Kvassman, J. O., and Shore, J. D. (1995) Purification of human plasminogen activator inhibitor (PAI-1) from *Escherichia coli* and

separation of its active and latent forms by hydrophobic interaction chromatography. *Fibrinolysis 9*, 215−221.
(39) Komissarov, A. A., Florova, G., and Idell, S. (2011) Effects of extracellular DNA on plasminogen activation and fibrinolysis. *J. Biol. Chem. 286*, 41949−41962.
(40) Komissarov, A. A., Stankowska, D., Krupa, A., Fudala, R., Florova, G., Florence, J., Fol, M., Allen, T. C., Idell, S., Matthay, M. A., and Kurdowska, A. K. (2012) Novel aspects of urokinase function in the injured lung: Role of α2-macroglobulin. *Am. J. Physiol. 303*, L1037−L1045.
(41) Komissarov, A. A., Declerck, P. J., and Shore, J. D. (2002) Mechanisms of conversion of plasminogen activator inhibitor 1 from a suicide inhibitor to a substrate by monoclonal antibodies. *J. Biol. Chem. 277*, 43858−43865.
(42) Komissarov, A. A., Declerck, P. J., and Shore, J. D. (2004) Protonation state of a single histidine residue contributes significantly to the kinetics of the reaction of plasminogen activator inhibitor-1 with tissue-type plasminogen activator. *J. Biol. Chem. 279*, 23007−23013.
(43) Verhamme, I., Kvassman, J. O., Day, D., Debrock, S., Vleugels, N., Declerck, P. J., and Shore, J. D. (1999) Accelerated conversion of human plasminogen activator inhibitor-1 to its latent form by antibody binding. *J. Biol. Chem. 274*, 17511−17517.
(44) Van De Craen, B., Scroyen, I., Vranckx, C., Compernolle, G., Lijnen, H. R., Declerck, P. J., and Gils, A. (2012) Maximal PAI-1 inhibition in vivo requires neutralizing antibodies that recognize and inhibit glycosylated PAI-1. *Thromb. Res. 129*, e126−e133.
(45) Jensen, J. K., Durand, M. K., Skeldal, S., Dupont, D. M., Bodker, J. S., Wind, T., and Andreasen, P. A. (2004) Construction of a plasminogen activator inhibitor-1 variant without measurable affinity to vitronectin but otherwise normal. *FEBS Lett. 556*, 175−179.
(46) Shore, J. D., Day, D. E., Francis-Chmura, A. M., Verhamme, I., Kvassman, J., Lawrence, D. A., and Ginsburg, D. (1995) A fluorescent probe study of plasminogen activator inhibitor-1. Evidence for reactive center loop insertion and its role in the inhibitory mechanism. *J. Biol. Chem. 270*, 5395−5398.
(47) Kvassman, J. O., Verhamme, I., and Shore, J. D. (1998) Inhibitory mechanism of serpins: Loop insertion forces acylation of plasminogen activator by plasminogen activator inhibitor-1. *Biochemistry 37*, 15491−15502.
(48) Lawrence, D. A., Olson, S. T., Muhammad, S., Day, D. E., Kvassman, J. O., Ginsburg, D., and Shore, J. D. (2000) Partitioning of serpin-proteinase reactions between stable inhibition and substrate cleavage is regulated by the rate of serpin reactive center loop insertion into β-sheet A. *J. Biol. Chem. 275*, 5839−5844.
(49) Schechter, I., and Berger, A. (1967) On the size of the active site in proteases. I. Papain. *Biochem. Biophys. Res. Commun. 27*, 157−162.
(50) Madison, E. L., Goldsmith, E. J., Gerard, R. D., Gething, M. J., Sambrook, J. F., and Bassel-Duby, R. S. (1990) Amino acid residues that affect interaction of tissue-type plasminogen activator with plasminogen activator inhibitor 1. *Proc. Natl. Acad. Sci. U.S.A. 87*, 3530−3533.
(51) Coombs, G. S., Bergstrom, R. C., Madison, E. L., and Corey, D. R. (1998) Directing sequence-specific proteolysis to new targets. The influence of loop size and target sequence on selective proteolysis by tissue-type plasminogen activator and urokinase-type plasminogen activator. *J. Biol. Chem. 273*, 4323−4328.
(52) Declerck, P. J., Alessi, M. C., Verstreken, M., Kruithof, E. K., Juhan-Vague, I., and Collen, D. (1988) Measurement of plasminogen activator inhibitor 1 in biologic fluids with a murine monoclonal antibody-based enzyme-linked immunosorbent assay. *Blood 71*, 220−225.
(53) Huber, K. (2001) Plasminogen activator inhibitor type-1 (part one): Basic mechanisms, regulation, and role for thromboembolic disease. *J. Thromb. Thrombolysis 11*, 183−193.
(54) Zeerleder, S., Schroeder, V., Hack, C. E., Kohler, H. P., and Wuillemin, W. A. (2006) TAFI and PAI-1 levels in human sepsis. *Thromb. Res. 118*, 205−212.
(55) Fay, W. P., Murphy, J. G., and Owen, W. G. (1996) High concentrations of active plasminogen activator inhibitor-1 in porcine coronary artery thrombi. *Arterioscler., Thromb., Vasc. Biol. 16*, 1277−1284.
(56) Naessens, D., Gils, A., Compernolle, G., and Declerck, P. J. (2003) Elucidation of the epitope of a latency-inducing antibody: Identification of a new molecular target for PAI-1 inhibition. *Thromb. Haemostasis 90*, 52−58.
(57) Andreasen, P. A. (2007) PAI-1: A potential therapeutic target in cancer. *Curr. Drug Targets 8*, 1030−1041.
(58) Huang, W. T., Vayalil, P. K., Miyata, T., Hagood, J., and Liu, R. M. (2012) Therapeutic value of small molecule inhibitor to plasminogen activator inhibitor-1 for lung fibrosis. *Am. J. Respir. Cell Mol. Biol. 46*, 87−95.
(59) Izuhara, Y., Yamaoka, N., Kodama, H., Dan, T., Takizawa, S., Hirayama, N., Meguro, K., van Ypersele de, S. C., and Miyata, T. (2010) A novel inhibitor of plasminogen activator inhibitor-1 provides antithrombotic benefits devoid of bleeding effect in nonhuman primates. *J. Cereb. Blood Flow Metab. 30*, 904−912.
(60) Aleman, C., Alegre, J., Monasterio, J., Segura, R. M., Armadans, L., Angles, A., Varela, E., Ruiz, E., and Fernandez, d. S. (2003) Association between inflammatory mediators and the fibrinolysis system in infectious pleural effusions. *Clinical Science 105*, 601−607.
(61) Green, J., Doughty, L., Kaplan, S. S., Sasser, H., and Carcillo, J. A. (2002) The tissue factor and plasminogen activator inhibitor type-1 response in pediatric sepsis-induced multiple organ failure. *Thromb. Haemostasis 87*, 218−223.
(62) Raeven, P., Feichtinger, G. A., Weixelbaumer, K. M., Atzenhofer, S., Redl, H., Van, G. M., Bahrami, S., and Osuchowski, M. F. (2012) Compartment-specific expression of plasminogen activator inhibitor-1 correlates with severity/outcome of murine polymicrobial sepsis. *Thromb. Res. 129*, e238−e245.
(63) Raaphorst, J., Johan Groeneveld, A. B., Bossink, A. W., and Erik, H. C. (2001) Early inhibition of activated fibrinolysis predicts microbial infection, shock and mortality in febrile medical patients. *Thromb. Haemostasis 86*, 543−549.
(64) Zeerleder, S., Hack, C. E., and Wuillemin, W. A. (2005) Disseminated intravascular coagulation in sepsis. *Chest 128*, 2864−2875.
(65) Madoiwa, S., Nunomiya, S., Ono, T., Shintani, Y., Ohmori, T., Mimuro, J., and Sakata, Y. (2006) Plasminogen activator inhibitor 1 promotes a poor prognosis in sepsis-induced disseminated intravascular coagulation. *Int. J. Hematol. 84*, 398−405.
(66) Shapiro, N. I., Schuetz, P., Yano, K., Sorasaki, M., Parikh, S. M., Jones, A. E., Trzeciak, S., Ngo, L., and Aird, W. C. (2010) The association of endothelial cell signaling, severity of illness, and organ dysfunction in sepsis. *Crit. Care 14*, R182.
(67) Seiffert, D., and Loskutoff, D. J. (1991) Kinetic analysis of the interaction between type 1 plasminogen activator inhibitor and vitronectin and evidence that the bovine inhibitor binds to a thrombin-derived amino-terminal fragment of bovine vitronectin. *Biochim. Biophys. Acta 1078*, 23−30.